Am J Cancer Res 2022;12(3):1241-1263
www.ajcr.us /ISSN:2156-6976/ajcr0142154

Original Article

FOXO3-dependent suppression of PD-L1 promotes anticancer immune responses via activation of natural killer cells

Young Min Chung[1,2], Wen Bin Tsai[1,3], Pragya P Khan[1], Jessica Ma[2], Jonathan S Berek[2], James W Larrick[1], Mickey C-T Hu[1,2]

[1]Panorama Institute of Molecular Medicine & Panorama Research Institute, Sunnyvale, CA 94089, USA; [2]Division of Gynecologic Oncology, Department of Obstetrics and Gynecology, Stanford University School of Medicine, Stanford, CA 94305, USA; [3]Department of Genomic Medicine, University of Texas M. D. Anderson Cancer Center, Houston, TX 77030, USA

Received February 3, 2022; Accepted February 24, 2022; Epub March 15, 2022; Published March 30, 2022

Abstract: Boosting anticancer immunity by blocking immune checkpoints such as the programmed death-1 (PD-1) or its ligand (PD-L1) is a breakthrough anticancer therapy. However, many cancer patients do not respond well to immune checkpoint blockades (ICBs) alone. Here we show that low-dose pharmacological immunoactivators (e.g., SN38, topotecan, sorafenib, etc.) notably downregulate PD-L1 and upregulate FOXO3 expression in various human and murine cancer cell lines. In a mouse tumor model, low-dose SN38 treatment markedly suppresses tumor growth, reduces PD-L1 expression, and enhances FOXO3 expression in primary tumor specimens. SN38 therapy engages the tumor-infiltrating mouse NK1.1/CD49b/NKG2D-positive natural killer (NK) cells to attack tumor cells by inducing mouse IFN-γ and granzyme-B secretion in the tumor microenvironment (TME) *in vivo*. SN38 treatment also promotes tumor cell apoptosis in the TME. SN38 treatment significantly decreases STAT3-pY705 and IL-6 protein levels; FOXO3 is essential for SN38-mediated PD-L1 downregulation. Collectively, these findings may contribute to future translational or clinical investigations tackling difficult-to-treat cancers with immune-activating medicines or combined with ICB immunotherapy.

Keywords: Cancer immunotherapy, antitumor immunity, immune checkpoint, PD-L1, FOXO3, natural killer cell, immunoactivator, SN38, topotecan, sorafenib

Introduction

Activating antitumor immunity by harnessing specific monoclonal antibody blockades against PD-1 or PD-L1 immune checkpoint is among the most promising antitumor therapies [1, 2]. The current knowledge of this therapeutic mechanism is that the PD-1/PD-L1 checkpoint suppresses cytotoxic T cells, and blockades against PD-1 or PD-L1 may resurrect cytotoxic T cells to tackle tumor cells and trigger the antitumor immune mechanism. However, single-agent anti-PD-1 or anti-PD-L1 antibodies may only display therapeutic efficacy in certain cancer patients, and a large number of cancer patients may be unresponsive or resistant to PD-1 or PD-L1 blockades. For instance, clinical investigations of PD-1 or PD-L1 blockades in those difficult-to-treat tumors exhibit poor responsive rates in these tumors. In addition, these blockades are limited in enhancing the survival rates of patients with these lethal tumors, which include glioblastoma [3], pancreatic cancer [4, 5], ovarian cancer (OvCa) [6], etc. Specifically, in patients with OvCa, clinical investigations of PD-1 or PD-L1 blockades alone indicate relatively disappointing results in terms of objective response rates (ORR: 6-15% only) [6]. The U.S. Food and Drug Administration (FDA) has not approved any PD-1 or PD-L1 blockades for treating patients with OvCa currently.

In general, recognizing tumor cells by cytotoxic T cells, mainly CD8+ T cells, is the major histocompatibility complex (MHC)-restricted and

requires tumor antigen presentation associated with MHC class I molecules on the cell surface of antigen-presenting cells [7, 8]. Recent findings show that tumor cells can escape from CD8+ T cell attacks by downregulating β2-microglobulin protein expression, leading to impaired MHC presentation [9]. In contrast, NK cells play pivotal roles in recognizing and attacking tumors as central innate immune cells to carry out antitumor immune surveillance and responses [10]. Unlike T cell recognition, NK cell recognition of tumor cells is not MHC restricted. Therefore, NK cells do not require prior priming with specific antigens for targeting tumor cells [10-12]. In addition, NK cells are early primary producers of cytokines, such as interferon-γ (IFN-γ), to influence crucial T-cell responses [13]. They can directly lyse tumor cells or other target cells through granzymes and perforin [14]. Therefore, engaging NK cells to attack tumor cells may strengthen ICB efficacy in antitumor immunotherapy.

A complex interplay between inhibitory and activating receptors regulates NK cell stimulation to trigger the recognition and killing of cancer cells [15]. The primary inhibitory receptors include killer cell immunoglobulin-like receptors (KIR), which recognize classical human leukocyte antigens (HLA) A/B/C, and the heterodimer CD94/NKG2A recognizes non-classical HLA-E. Both NKG2A and NKG2C recognize HLA-E with different affinities leading to inhibition and activation, respectively [16]. The central stimulatory receptors include stress-induced ligands (e.g., NKG2D on NK cells recognizing MICA/B, ULBP), antibody-coated cells (e.g., the Fc receptor CD16 on NK cells recognizing the Fc portion of IgG1 bound to target cells), and natural cytotoxicity receptors (e.g., NKp30, NKp44, and NKp46 on human NK cells). In addition to cytotoxic T cells (such as CD8+ T cells) expressing immune checkpoint PD-1 protein [17], tumor-specific NK cells also express PD-1 receptor on the cell surface and blocking PD-1 with anti-PD-1 antibody triggers NK cells to infiltrate and destroy tumors in animal models [18, 19]. These intriguing findings discover that activated NK cells (having more responsive phenotypes) express significantly higher levels of PD-1 than inactive NK cells (showing exhausted phenotypes). This discovery implies that significant suppression of NK cell-engaged anticancer immunity *in vivo* may occur through the PD-1 checkpoint inhibitory mechanism. In addition, different clinical investigations have assessed the efficacy of direct NK cell-based therapies in cancer patients [20, 21]. Although the results are encouraging in hematological malignancies, clinical benefits are not very promising in solid tumors [20, 21].

Previously we have identified anticancer pharmacological agents, SN38 (an irinotecan analog) and metformin, that can promote the reprogramming of human OvCa and breast cancer (BCa) cells into their benign perspective cells [22] through activation of FOXO3. FOXO3 is a key transcription factor that controls the transcription of many genes crucial for regulating cell-cycle control, DNA damage response, oxidative and other stress, aging and longevity, apoptosis and autophagy, and tumor suppression networks in humans and animal cells [23-29]. Thus, we further deciphered the signaling pathways regulating antitumor effects on tumors treated with low doses of SN38 *in vivo*. Unexpectedly, we found that treating the tumor-bearing mice with a low amount of SN38 (5 μg/kg body weight), whose cytotoxicity was minimal in human ovarian tumors, nonetheless markedly reduced tumor volume in a mouse model. Therefore, we were skeptical that low-dose SN38's inconsequential cytotoxicity could significantly inhibit ovarian tumor survival and progression *in vivo*. Instead, we hypothesized that a disparate system (for instance, an anticancer immune system) would plausibly cause the outcome. Notably, our previous findings have demonstrated that low-dose SN38 or other FDA-approved small-molecule medicines can potently decrease c-Myc protein expression in a FOXO3-dependent manner [22, 30]. Moreover, recent findings indicate that increased of c-Myc protein expression is significantly associated with the protein level of PD-L1 in primary human tumor specimens from patients with lung cancer [31]. Based mainly on these preconceptions, we evaluated the effect of low-dose SN38 or topotecan or other anticancer small-molecule medications on regulating the expression of PD-L1 and FOXO3, as well as low-dose SN38-mediated *in vivo* anticancer immune responses in a mouse model with human cancer. Here we show that low-dose SN38 notably fosters FOXO3-dependent suppression of PD-L1 expression in human tumor cells, potently suppresses tumor progression and recruits mouse NK1.1/CD49b/NKG2D-positive NK cells into the tumor microenviron-

ment (TME). Our results reveal a novel immunological mechanism underlying SN38-induced engagement of NK cells infiltrating human tumors and triggering an NK cell-mediated antitumor immune response through promoting IFN-γ and granzyme-B secretion in the TME. We have proposed the anticipated therapeutic significance and clinical applications of this novel NK cell mechanism in improving overarching cancer immunotherapy.

Methods and materials

Antibodies and reagents

For immunofluorescence analysis, the following primary antibodies (Abs) were purchased and used (1:1000 dilution): Abs against FOXO3a [Cell Signaling Technology (CST), 2497], FOXO3a (Abcam, ab53287, clone EP1949Y), FOXO3 (FKHRL1) [Santa Cruz Biotechnology (SCBT), sc-9813, N-16], PD-L1 (CST, 13684), PD-L1 (R&D Systems, MAB1561), PD-L1 [Thermo Fisher Scientific (TFS), 14-5983-82], PD-L1 (TFS, PA5-20343), PD-L1 (TFS, eBioscience, clone MIH1), c-Myc (MilliporeSigma, 06-340), STAT3-pY705 (SCBT, sc-8059), IL-6 (Abcam, ab6672), FITC-conjugated CD49b (BioLegend, 108906), FITC-conjugated NK1.1 (BioLegend, 108706), Alexa-594-conjugated CD3 (BioLegend, 100240), Alexa-594-conjugated CD8 (BioLegend, 100758), IFN-γ (BioLegend, 505802), NKG2D (Bioss Antibodies, bs-0938R), Granzyme B (SCBT, sc-8022). The following secondary Abs were purchased and used (1:200 dilution): Alexa Fluor 488 Chicken anti-Rat (TFS, A-21470), Alexa Fluor 647 Chicken anti-mouse (TFS, A-21463), Alexa Fluor 594 Chicken anti-goat (TFS, A-21468), Alexa Fluor 594 Donkey anti-rabbit (TFS, A-21207), Alexa Fluor 488 goat anti-mouse (TFS, A-11001), Alexa Fluor 594 Donkey anti-rabbit (TFS, A-21207). For immunoblotting analysis, the following primary Abs were purchased and used: FOXO3 (Abcam, ab53287), PD-L1 (CST, 13684) p27Kip1 (BD Pharmingen, 554069), GAPDH (TFS, MA5-15738), STAT3-pY705 (SCBT, sc-8059), c-Myc (SCBT, sc-764) NKG2D (Bioss Antibodies, bs-0938R), NKp44 [Biorbyt LLC (St Louis, MO), orb315559], and NKp46 (M-100) (SCBT, sc-292796). The following secondary Abs were purchased and used (1:3000 dilution): horseradish peroxidase-conjugated donkey anti-mouse IgG (H+L) (715-035-150) and donkey anti-rabbit IgG (H+L) (711-035-152) Abs [Jackson ImmunoResearch (West Grove, PA)]. For animal studies, InVivoMAb anti-mouse PD-1 mAb (Bio X Cell, BE0146) was purchased from Bio X Cell. Pharmacological agents or solvents: SN38 (7-ethyl-10-hydroxycamptothecin) was purchased from Fisher Scientific (Pittsburgh, PA) or MedKoo Biosciences, Inc. (Morrisville, NC). Metformin was purchased from Fisher Scientific or Cayman Chemical (Ann Arbor, Michigan). Olaparib was obtained from LC Laboratories (Woburn, MA). Dimethylsulfoxide (DMSO) and methanol were purchased from Sigma (St. Louis, MO). SN38 was dissolved in DMSO and metformin was dissolved in sterile H_2O or DMSO.

Cell culture and cell lines

All cell lines were grown at 37°C and 5% CO_2 in DMEM/F12 supplemented with L-glutamine, penicilline/streptomycin and 10% fetal bovine serum (FBS). Mouse ID8 and ID8-Luc OvCa cell lines were kindly provided by Oliver Dorigo, Division of Gynecologic Oncology, Stanford University School of Medicine. Mouse metastatic 4T1 and 4T1-Luc BCa cell lines were kindly provided by Xiaoyuan (Shawn) Chen, Laboratory of Molecular Imaging and Nanomedicine, National Institutes of Health (NIH). OVCA429, an established cell line derived from a patient with late-stage serous OvCa, was kindly provided by Robert C. Bast, Jr., Division of Cancer Medicine, University of Texas MD Anderson Cancer Center. MDA-MB-231, BT-549, MCF-7, SKBR3 BCa cell line and NK-92 cell line were obtained from the American Type Culture Collection. For generating stable cell lines, four HuSH 29mer shRNA constructs against human FOXO3 (NM_001455) and control HuSH shRNA cloning vector (pRS) using U6 promoter were purchased from Origene (Rockville, MD). OVCA429 cells were transfected with a combination of four HuSH 29mer shRNA constructs concurrently or control pRS vector by liposome using GenJet™ In Vitro DNA Transfection Reagent (SignaGen Laboratories, Gaithersburg, MD). After puromycin selection (1 μg/ml), the OVCA429 FOXO3-knockdown pooled stable clones (designated OVCA429-FOXO3-shRNA) and the vector control stable clones (designated OVCA429-Control-shRNA) were selected.

Flow cytometry analysis

Cells were trypsinized, aliquoted (3×10^5 cells per condition) and fixed for 15 minutes in 4%

(v/v, in PBS) paraformaldehyde (Electron Microscopy Sciences) at room temperature. For intracellular staining, cells were permeabilized by adding ice-cold 100% methanol slowly to pre-chilled cells, while gently vortexing (to a final concentration of 90% methanol) and incubated at 4°C for 30 min. Then, cells were washed in PBS, centrifuged at 1200 g, and resuspended in PBS with 3% BSA (staining buffer). For immunostaining, cells were incubated in staining buffer containing a primary Ab specific to PD-L1 (CST, 13684), or FOXO3 (Abcam, ab53287) (1:200 dilution) or control rabbit IgG for 1 h at room temperature. After washing three times with PBS, cells were incubated in staining buffer containing a FITC-conjugated anti-rabbit (1:200 dilution) secondary Ab (Jackson ImmunoResearch) for 30 min at room temperature in the dark. Subsequently, cells were characterized using a FACScan flow cytometer (BD Biosciences) at the Institutional shared flow cytometry facility. Ten thousand events were collected in each run. The data were analyzed by FlowJo software.

Immunofluorescence analysis

For cancer cell staining, cells were cultured on glass coverslips for 24 h. After treatments with SN38 (10 nM) or other pharmacological drugs [metformin (10 or 100 μM) or Olaparib (1 or 10 μM)] and vehicle (H_2O or DMSO) for 24 h, cells were fixed with 4% paraformaldehyde for 10 min and permeabilized with 0.1% Triton X-100 solution in phosphate-buffered saline (PBS). Cells on glass coverslips were washed with PBS and blocked with PBS containing 0.1% Triton X-100 and 10% normal horse serum, incubated with a primary Ab specific to FOXO3 or PD-L1 or the indicated proteins (1:50 to 1:100 dilution) for 2 h at room temperature, followed by Alexa 594 (red)-conjugated anti-rabbit (1:50 dilution or 1:100 dilution) and Alexa 488 (green)-conjugated anti-mouse (1:100 dilution) secondary Abs (Thermo Fisher Scientific). Cells were counterstained with DAPI solution (Sigma) to show the nuclei. For tumor tissue staining, tissues were rapidly frozen in the Tissue-Plus® O.C.T. Compound Embedding medium (Scigen, 4583) at -80°C. Tissue sections of tumor were cut at 5 μm thickness using a Thermo Scientific Shandon Cryotome E. The tissue slides were permeabilized with 0.1% Triton X-100 solution and blocked with the blocking solution, 10% normal horse serum and 5% bovine serum albumin (BSA), for 1 h at room temperature. Then, the slides were incubated with primary Abs against FOXO3 or PD-L1 or NK1.1 or CD3 or CD49b or CD8a or IFN-γ or IL-6 or the indicated proteins for 2 h at room temperature. After washing three times with PBS containing 0.1% Tween-20, secondary Abs (as described above) were added onto the slides for 20 min at room temperature. After staining with DAPI solution, the slides were washed three times with PBS containing 0.1% Tween-20 and mounted onto microscope slides with DABCO-glycerol antifade solution. Specific staining was visualized and fluorescence images were captured with a Zeiss LSM 880 Laser Scanning Confocal Microscope. To perform quantitative analyses of the relative expressions of individual proteins, we measured fluorescence intensities of individual fluorescence images using ImageJ (Ver. 1.53c). Based on three independent individual intensities, from which we constructed a histogram and determined the mean values of relative intensities as the integrated densities of individual proteins. Each error bar presented is the mean of standard deviation (SD).

Immunoblotting analysis

Cells were washed twice with PBS and lysed with lysis buffer containing protease ors at 4°C for 20 min. The lysates were centrifuged at 16,000 g for 10 min to remove cell debris, and total protein concentration was determined. The protein samples were subjected to SDS-PAGE and transferred onto nitrocellulose membranes (Bio-Rad). Membranes were blocked for 1 h in 3% BSA in Tris-buffered saline containing 0.1% Tween-20 (TBST) and incubated for 1 h with primary antibody diluted in TBST containing 1% BSA. After three washes with TBST, membranes were incubated for 1 h with horseradish peroxidase-conjugated secondary antibodies (1:3,000 or 1:5,000 dilution) in TBST containing 3% BSA. The immunoblots (or western blots) were visualized by an enhanced chemiluminescence kit obtained from Thermo Fisher Scientific or West-Q ECL Platinum Solution obtained from GenDEPOT (Barker, TX).

siRNA transfection

Human OVCA429 cells were maintained in DMEM/F12 media supplemented with 10% FBS, 3% L-glutamine, and 1% streptomycin/penicillin at 37°C in a humidified incubator con-

taining 5% CO_2 in the air. Human FOXO3a-siRNA-1 (sc-37887) and control-siRNA (sc-37007) were obtained from Santa Cruz Biotechnology. Human FOXO3-siRNA-2 (Hs01_00-119127) was obtained from Sigma-Aldrich. According to the manufacturer's instructions, cells were transfected with FOXO3-siRNA or control-siRNA using DharmaFECT 1 transfection reagent (Thermo Fisher Scientific, Rockford, IL, USA) and as described previously [28].

Animal studies

For tumor xenograft mouse models, female athymic nude mice were purchased from Charles River Laboratories, Inc. (Wilmington, MA) and maintained aseptically in an athymic animal room. For tumor-cell implantation, OVCA429 cells (in log-phase growth) were harvested, washed with sterile PBS, and re-suspended in PBS. Then, cells [3×10^6/mouse in 0.1 ml PBS with 30% extracellular matrix (ECM) gel (Sigma)] were injected subcutaneously into the flank of each mouse as described previously [22, 26, 30]. When palpable solid tumors were detected (approximately 100 mm^3), mice from each treatment group (n=5/group) were given an intravenous injection (0.1 ml) of SN38 (5 or 50 μg/kg body weight (BW)/mouse) or equal amount of control (10% DMSO) once every three days for 35 days. The tumor sizes were measured twice per week with a Vernier caliper. Data are presented as means and standard deviations (SD) of five mice in each group. All mice were weighed twice per week as a measure of overall systemic toxicity. After euthanasia, the tumor tissues were resected from the treated mice and tissue slides were prepared for immunofluorescence or immunoblotting analysis. All procedures were performed in compliance with the guidelines and regulations of the Institutional Animal Care and Use Committee (IACUC).

Statistical analysis

All data are presented as means and SD from at least three independent experiments. The statistical significance of differences in expressions of proteins examined in cells and the percentage of tumor growth or cell survival or animal survival between two groups were analyzed with two-sided unpaired Student's *t*-tests with GraphPad PRISM (Ver. 8) statistical software (San Diego, CA) or Excel (Microsoft Office). Animal survival analysis was performed by the Kaplan-Meier method using GraphPad PRISM (Ver. 8). All statistical tests were two-sided, and *P* values less than 0.05 were considered statistically significant.

Results

Because we hypothesized that an anticancer immune response could cause the suppression of tumor growth by low-dose SN38, we set out to determine whether SN38 plays a significant role in regulating PD-L1 and FOXO3 expression in ovarian cancer (OvCa) and breast cancer (BCa) cell lines. We treated four human OVCA429 (OvCa), MDA-MB-231 (BCa), MCF-7 (BCa), and BT-549 (BCa) cell lines with low doses of SN-38 and negative control [dimethyl sulfoxide (DMSO)]. We determined the expression levels of PD-L1 and FOXO3 in these cells using three independent protein expression analyses, including immunoblotting (**Figure 1A**), flow cytometry (**Figure 1B**), and immunofluorescence analysis (**Figure 1C-E**). Our data showed that low doses of SN38 downregulated PD-L1 and upregulated FOXO3 expression significantly in these cells compared with control. In addition, we showed that low doses of SN38 enhanced FOXO3 expression and reduced PD-L1, cyclin D1, and interleukin-6 (IL-6) expression significantly in mouse 4T1 (BCa) (**Figure 1F**).

Next, we examined the effects of other pharmacological drugs on regulating PD-L1 and FOXO3 expression in OvCa and BCa cells. Our results indicated that topotecan, an FDA-approved clinically-used drug, downregulated PD-L1 and upregulated FOXO3 expression significantly in mouse ID-8 cells compared with control (DMSO) in a dose-dependent manner using immunoblotting analysis (**Figure 2A**). Similarly, topotecan (0.5 μM) decreased PD-L1 expression significantly in ID-8 cells compared with control using flow cytometry (**Figure 2B**). A clinically-used anticancer drug, Sorafenib, reduced PD-L1 and increased FOXO3 expression significantly in OVCA429 cells compared with control in a dose-dependent manner using immunoblotting analysis (**Figure 2C**). Using flow cytometry, we confirmed that sorafenib (2.5 μM) significantly suppressed PD-L1 expression in OVCA429 cells compared with control (**Figure 2D**). In addition, we assessed the effects of seven different pharmacological drugs on regu-

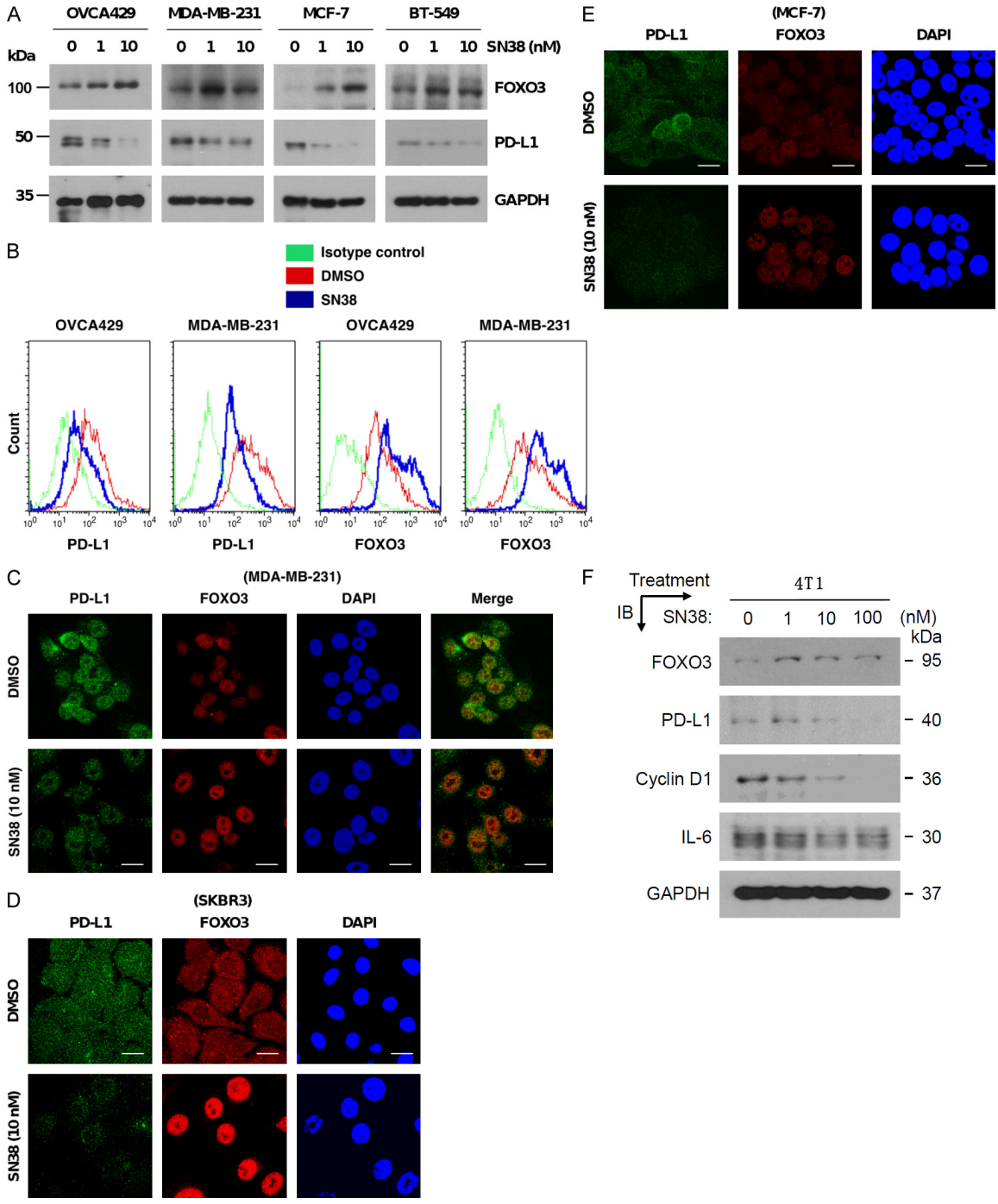

Figure 1. Low doses of SN38 downregulate PD-L1 and upregulate FOXO3 expression in cancer cell lines. A. We analyzed the total lysates of the human breast cancer (BCa) and ovarian cancer (OvCa) cell lines treated with different low doses of SN38 or equal amounts of dimethyl sulfoxide (DMSO) (denoted as 0 nM) using immunoblotting (IB) with the designated antibodies. B. We treated OVCA429 (OvCa) or MDA-MB-231 (BCa) cells with low-dose SN38 (10 nM) or DMSO control and analyzed these cells using flow cytometry with the designated antibodies or isotype-matched IgG control. C-E. We incubated cell slides of the indicated human tumor cells treated with SN38 or DMSO with an anti-human PD-L1 or anti-human FOXO3 antibody followed by a specific Alexa-Fluor secondary antibody and fluorescence confocal microscopy (FCM). We utilized DAPI to show the nuclei. F. We analyzed the total lysates of mouse 4T1 metastatic BCa cells treated with various doses of SN38 or DMSO (denoted as 0 nM) using IB with the designated antibodies described above.

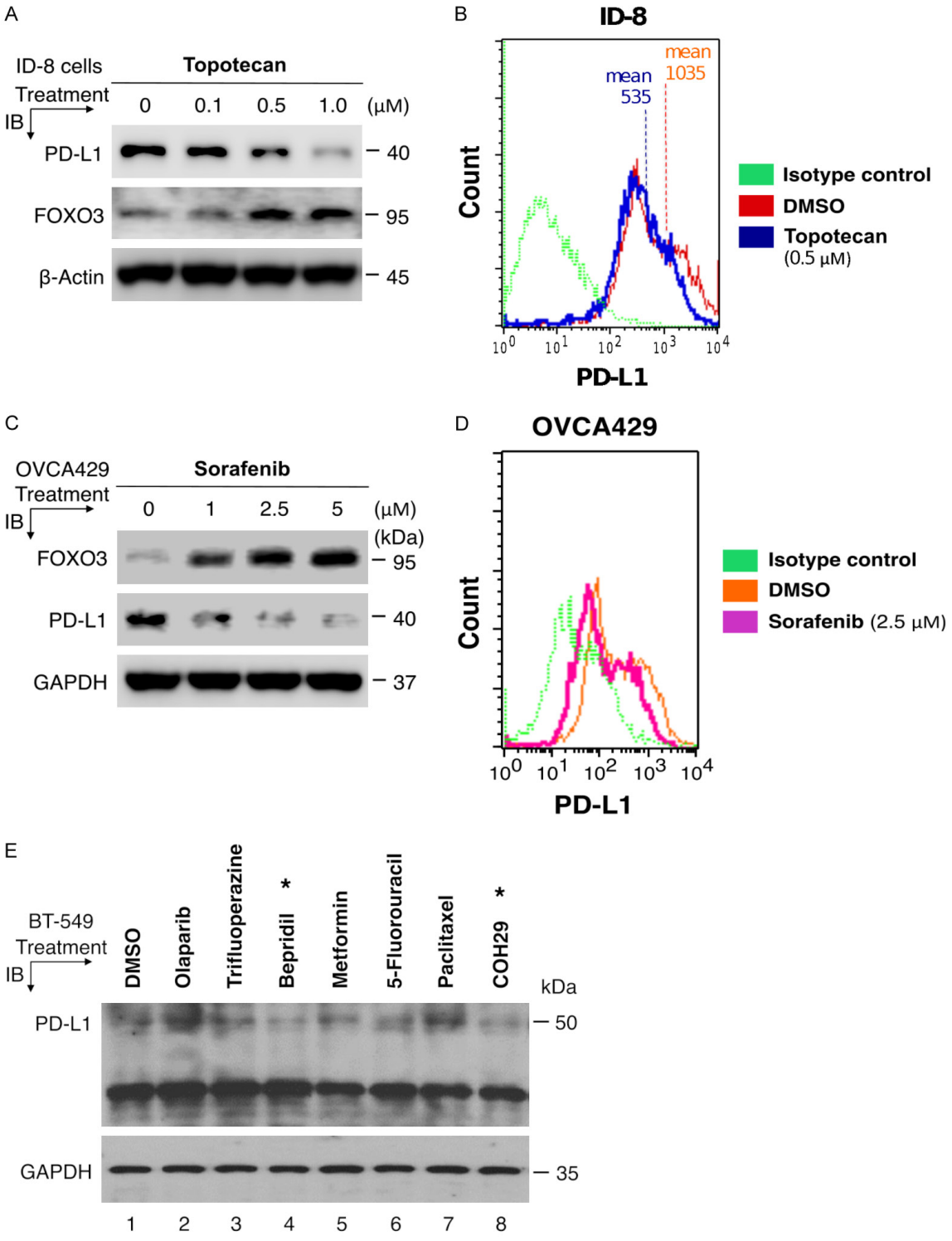

Figure 2. Other pharmacological drugs downregulate PD-L1 and upregulate FOXO3 expression in tumor cells. A. We analyzed the total lysates of the mouse ID-8 OvCa cells treated with different low doses of topotecan or equal amounts of DMSO (denoted as 0 nM) as indicated using immunoblotting (IB) with the designated antibodies. B. We treated ID-8 cells with topotecan (0.5 μM) or DMSO control and analyzed these cells by flow cytometry with the designated antibodies or isotype-matched IgG control. C. We analyzed the total lysates of OVCA429 cells treated with the indicated doses of Sorafenib or DMSO (denoted as 0 nM) using IB with the designated antibodies. D. We treated OVCA429 cells with Sorafenib (2.5 μM) or DMSO control and analyzed these cells by flow cytometry with the designated antibodies or isotype-matched IgG control. E. We treated human BT-549 BCa cells with DMSO (control) or the indicated drugs (10 μM/each) except Metformin and 5-Fluorouracil (100 μM/each). We analyzed the total lysates of cells using IB with specific antibodies as indicated. GAPDH represents the loading controls.

lating PD-L1 expression in human BCa cells using immunoblotting analysis. Six medicines are FDA-approved (olaparib, trifluoperazine, bepridil, metformin, 5-fluorouracil, and paclitaxel), and one (COH29) is under clinical investigation. Our data showed that bepridil and COH29 (10 μM/each) could significantly reduce PD-L1 expression in BT-549 cells compared with control (**Figure 2E**).

Using a tumor mouse model, we demonstrated that intravenous (i.v.) administration of low doses of SN38 (5 or 50 μg/kg BW) markedly suppressed (more than 60% or 95% suppression, respectively) OVCA429 tumor growth in the mouse tumor model *in vivo* compared with control (DMSO) (**Figure 3A**). Unexpectedly, administration of SN38 at a very low-dose (5 μg/kg BW) still exhibited a significant tumor-suppressive effect, suggesting that an alternative mechanism such as tumor-specific immunity may result in low-dose SN38-mediated tumor suppression. Thus, we investigated whether low-dose SN38 regulated the expression of PD-L1 and FOXO3 in primary OVCA429 tumor cells *in vivo*. We resected the primary tumor tissues from the treated mice as described above. Then, we examined the protein expression of PD-L1 and FOXO3 in these tumor specimens using immunofluorescence analysis with anti-PD-L1 and anti-FOXO3 Abs and analyzed the stained cells by confocal microscope. Our results indicated that low-dose SN38 significantly promoted the protein level of nuclear FOXO3 and potently decreased the protein expression of PD-L1 in tumor cells treated with SN38 compared with DMSO-treated tumor tissues (**Figure 3B-E**). As antibody-negative controls, the data of tumor specimens stained with Alexa Fluor 488- or 594-conjugated secondary antibodies alone showed negative immunofluorescence signals (**Figure 3F**). After repeating these experiments for independent runs, the results were reproducible. These findings suggest that low-dose SN38 markedly enhances the nuclear FOXO3 expression and suppresses PD-L1 expression in tumor cells to block the PD-L1/PD-1 checkpoint, resulting in tumor suppression *in vivo*.

Next, we investigated whether SN38 treatment promotes NK cells or cytotoxic T lymphocytes (CTL) infiltrating into the TME after reducing the tumor PD-L1 levels in the mouse tumor model (**Figure 3A**). Thus, we evaluated mouse NK1.1 and CD3 protein expression in primary OVCA-429 tumor tissues using the same immunofluorescence analysis with anti-mouse NK1.1 and anti-mouse CD3 antibodies as described above. Our results revealed that most tumor-infiltrating immune cells were NK1.1-positive and CD3-negative in tumor specimens treated with low-dose SN38 compared with DMSO-treated tumor specimens (**Figure 4A-C**). Comparably, the tumor-infiltrating cytotoxic immune cells were predominantly CD49b-positive/CD3-negative in tumor specimens treated with SN38 (**Figure 4D-F**). These results suggest that the observed tumor-infiltrating mouse cytotoxic effector cells primarily be NK cells. In addition, we examined the protein expression of mouse NKG2D (m-NKG2D) and human leukocyte antigen (HLA) in primary OVCA429 tumor tissues using immunofluorescence analysis with anti-m-NKG2D antibody and measured the stained cells by confocal microscope. Indeed, our data displayed a significant increase of m-NKG2D-positive tumor-infiltrating mouse NK cells and a significant decrease of HLA-positive human tumor cells in tumor specimens treated with low-dose SN38 compared with DMSO-treated tumor samples (**Figure 5A-D**). As antibody-negative controls, the results of tumor specimens stained with Alexa Fluor 488- or 594-conjugated secondary antibodies alone showed negative immunofluorescence signals (**Figure 5E**). Accumulatively, our findings suggest that low-dose SN38 can engage NK1.1/CD49b/NKG2D-positive NK cells permeating the TME and suppressing tumor cell survival *in vivo*.

Since NK cells are potent producers of cytokines, particularly IFN-γ, which plays a crucial role in stimulating an antitumor immune response, we determined whether low-dose SN38 triggered NK cells producing mouse IFN-γ (m-IFN-γ) in the TME of OVCA429 tumors in mice *in vivo*. We used immunofluorescence analysis with antibodies against m-IFN-γ and m-NKG2D on OVCA429 tumor samples. Our results showed that low-dose SN38 significantly induced m-IFN-γ protein production together with increased m-NKG2D-positive NK cells in the TME of primary tumor specimens *in vivo* (**Figure 6A-D**). Similarly, we assessed whether low-dose SN38 triggered NK cells producing mouse granzyme B (m-granzyme B) in the TME of OVCA429 tumors in mice *in vivo*. Granzyme B is an NK cell-produced cytotoxic serum prote-

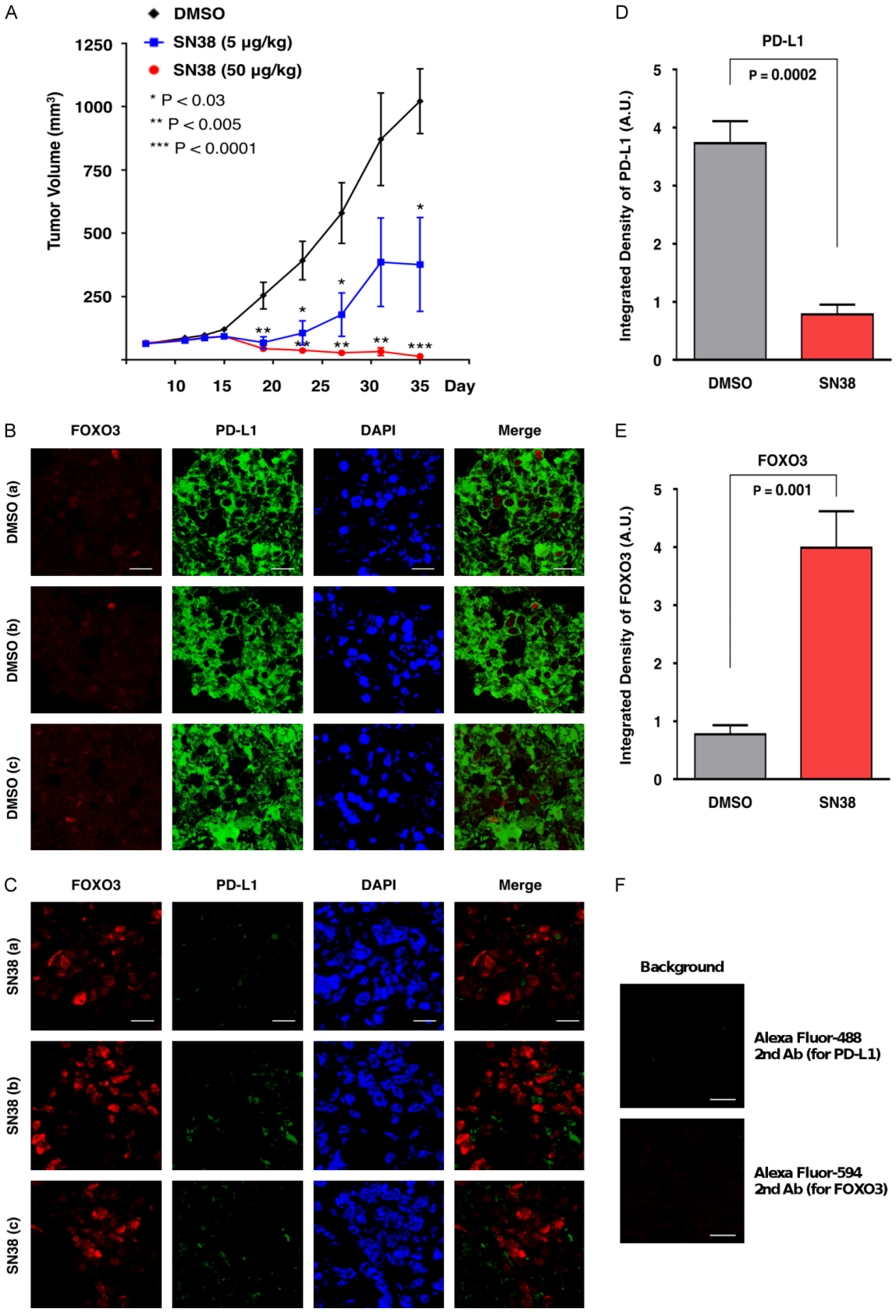
A
DMSO
SN38 (5 μg/kg)
SN38 (50 μg/kg)
* P < 0.03
** P < 0.005
*** P < 0.0001
Tumor Volume (mm³)
1250
1000
750
500
250
10
15
20
25
30
35
Day
D
PD-L1
P = 0.0002
Integrated Density of PD-L1 (A.U.)
5
4
3
2
1
0
DMSO
SN38
B
FOXO3
PD-L1
DAPI
Merge
DMSO (a)
DMSO (b)
DMSO (c)
E
FOXO3
P = 0.001
Integrated Density of FOXO3 (A.U.)
5
4
3
2
1
0
DMSO
SN38
C
FOXO3
PD-L1
DAPI
Merge
SN38 (a)
SN38 (b)
SN38 (c)
F
Background
Alexa Fluor-488
2nd Ab (for PD-L1)
Alexa Fluor-594
2nd Ab (for FOXO3)

Figure 3. Low doses of SN38 markedly suppress tumor growth in a mouse tumor model *in vivo*, regulate PD-L1 and FOXO3 expression in tumor cells. (A) We injected OVCA429 cells into female nude mice subcutaneously (n=5/group). When we detected palpable solid tumors (on day-10), we gave the mice an intravenous injection of SN38 [5 or 50 μg/kg body weight (BW)] or an equal amount of negative control, DMSO, once every three days for 35 days. The error bars denote standard deviation (SD), and the statistical test is the unpaired t-test. However, some error bars are tiny, so they are not evident on the graph. (B) We excised the tumor tissues from the treated mice (A), and prepared tissue slides for immunofluorescence (IF) analysis. Three slides of samples from tumors treated with DMSO were incubated with anti-FOXO3 or ant-PD-L1 antibodies, followed by an Alexa Fluor 594- or 488-conjugated secondary antibodies and FCM. We utilized DAPI to show the nuclei. Scale bar: 20 μm. A.U., arbitrary unit. (C) Similarly, three slides of samples from tumors treated with SN38 were incubated with anti-FOXO3 or ant-PD-L1 antibodies, followed by corresponding secondary antibodies and FCM as described above. (D, E) We showed the relative expressions of PD-L1 and FOXO3 between tumors treated with DMSO and SN38 *in vivo* in the histograms as indicated, respectively. (F) As negative antibody controls, we incubated slides of tumor specimens treated with DMSO (described above) with an Alexa Fluor 488- or 594-conjugated secondary antibody only and analyzed by FCM.

ase that plays a vital role in inducing the cellular apoptosis of tumor cells. We used immunofluorescence analysis with antibodies against m-granzyme B and m-NKG2D on OVCA429 tumor samples. Indeed, our data demonstrated that low-dose SN38 markedly increased m-granzyme B protein production and m-NKG2D-positive NK cells concurrently in the TME of primary tumor specimens *in vivo* (**Figure 6E-H**). Together, these findings suggest that low-dose SN38 therapy can trigger tumor-infiltrating NK1.1/CD49b/NKG2D-positive NK cells to suppress human tumor cells by inducing IFN-γ and granzyme-B secretion in the TME *in vivo.*

To evaluate whether FOXO3 is essential for regulating the SN38-mediated suppression of the expression of PD-L1 in human tumor cells, we effectively silenced FOXO3 expression in OVCA429 cells using transfection with two independent siRNAs targeting human FOXO3. Our results showed that silencing of FOXO3 expression in OVCA429 tumor cells significantly induced PD-L1 protein expression using immunoblotting and flow cytometric analyses with designated antibodies (**Figure 7A-C**). In addition, we transfected OVCA429 cells with FOXO3-shRNA (FOXO3-knockdown) or Control-shRNA (negative control) to generate stable cell lines. After the low-dose SN38 or DMSO (control) treatments, we performed immunofluorescence analysis using indicated antibodies. Notably, our data displayed that stably silencing of FOXO3 expression in OVCA429 tumor cells overrode downregulation of PD-L1 protein expression after SN38 treatment (**Figure 7D**, **7E**). These data were reproducible after repeating the experiments using different antibodies against human FOXO3 and PD-L1 from divergent sources (data not shown). These results suggest that FOXO3 is essential for SN38-mediated downregulation of PD-L1 expression in tumor cells.

Next, we deciphered the signaling mechanisms underlying the low-dose SN38-mediated suppression of tumor progression in tumor-bearing mice *in vivo*. Thus, we examined whether low-dose SN38 treatments regulated the expression levels of phosphor-STAT3 (STAT3-pY705) and interleukin (IL)-6, both of which play critical roles in modulating the expression of PD-L1 in tumor cells [32, 33]. Using immunofluorescence analysis on primary OVCA429 tumor tissues with specific antibodies against human STAT3-pY705 and HLA as designated, we showed that low-dose SN38 treatments markedly decreased STAT3-pY705 expression in HLA-positive human OVCA429 tumor cells *in vivo* (**Figure 8A-C**). Similarly, using specific antibodies against human IL-6 and HLA as indicated, we exhibited that low-dose SN38 treatments potently reduced IL-6 expression in HLA-positive human tumor cells *in vivo* (**Figure 8D-F**).

In addition, we assessed whether human tumor cells were subjected to NK cell-triggered apoptosis in the TME by using immunofluorescence analysis on OVCA429 tumor specimens with specific antibodies against cleaved PARP1 (a hallmark of apoptosis) [34, 35] and HLA as designated. Our data indicated a significant increase of cleaved PARP1 protein levels and a significant decrease of HLA-positive human tumor cells in OVCA429 tumor specimens treated with low-dose SN38 compared with DMSO-treated tumor samples (**Figure 9A-D**). Moreover, we confirmed the protein expression levels of STAT3, c-Myc, FOXO3, and PD-L1 in lysates of the primary OVCA429 tumor tissues by using

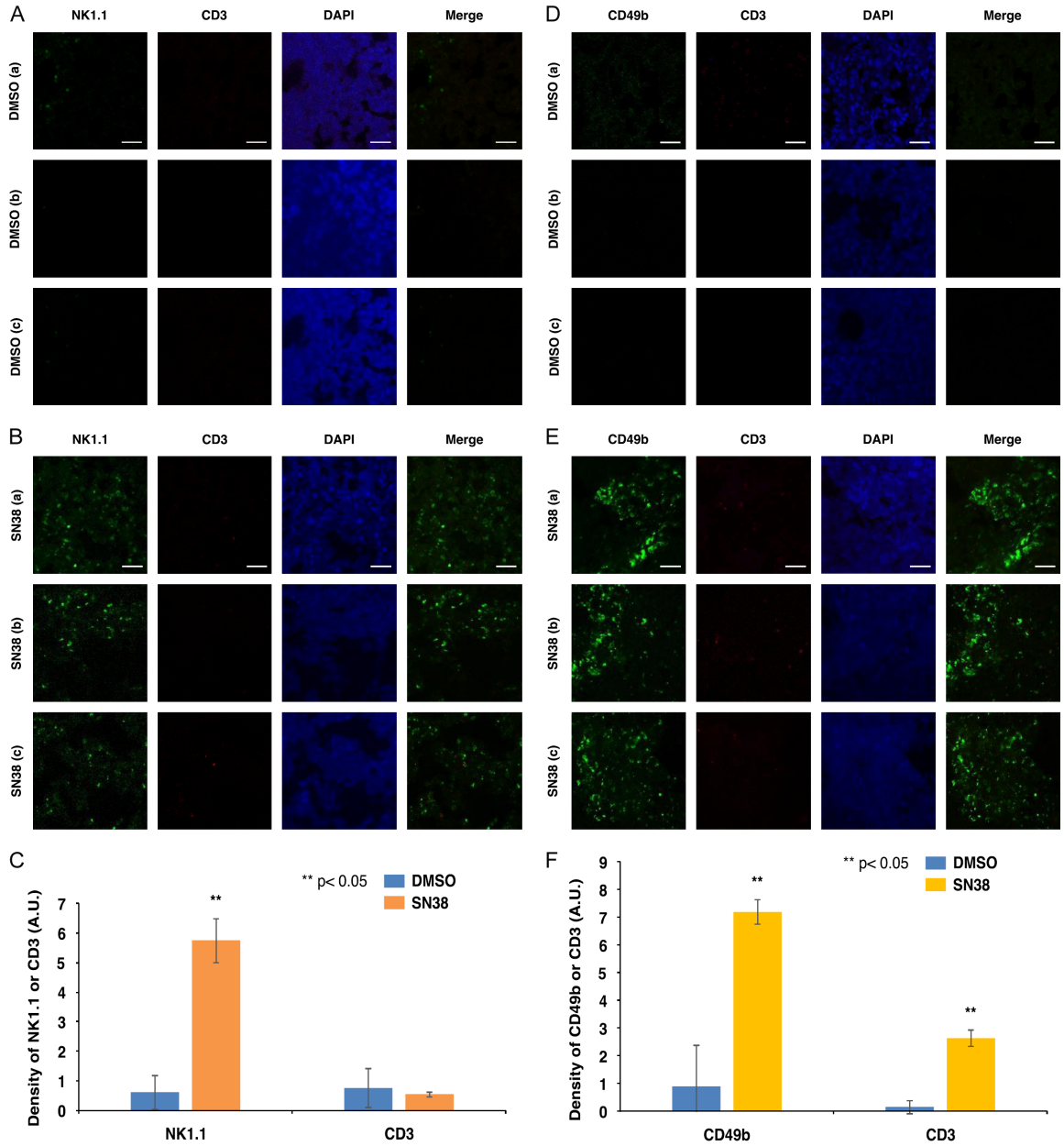

Figure 4. Low-dose SN38 triggers mouse NK1.1- and CD49b-positive NK cells infiltration into the tumor microenvironment (TME) *in vivo*. We prepared the tumor slides as described above (**Figure 3B**). (A) Three slides of samples from OVCA429 tumors treated with DMSO were incubated with anti-mouse NK1.1 or anti-mouse CD3 antibodies, followed by an Alexa Fluor 488- or 594-conjugated secondary antibodies and FCM. We utilized DAPI to show the nuclei. Scale bar: 20 μm. (B) Similarly, we incubated three slides of SN38-treated tumor specimens with anti-mouse NK1.1 or anti-mouse CD3 antibodies and analyzed the stained cells as described above. (C) We show the relative expressions of mouse NK1.1 and CD3 between tumors treated with DMSO and SN38 *in vivo* in the indicated histograms. (D, E) Three slides of samples from tumors treated with DMSO (D) or SN38 (E) were incubated with anti-mouse CD49b or anti-mouse CD3 antibodies, and the stained cells were analyzed as described. (F) The relative expressions of mouse CD49b and CD3 between tumors treated with DMSO and SN38 *in vivo* are shown in the indicated histograms, respectively.

immunoblotting analysis with specific antibodies against these proteins as indicated. Our data validated that low-dose SN38 treatments markedly diminished STAT3, c-Myc, and PD-L1 protein levels, while SN38 induced FOXO3 protein levels in OVCA429 tumor specimens

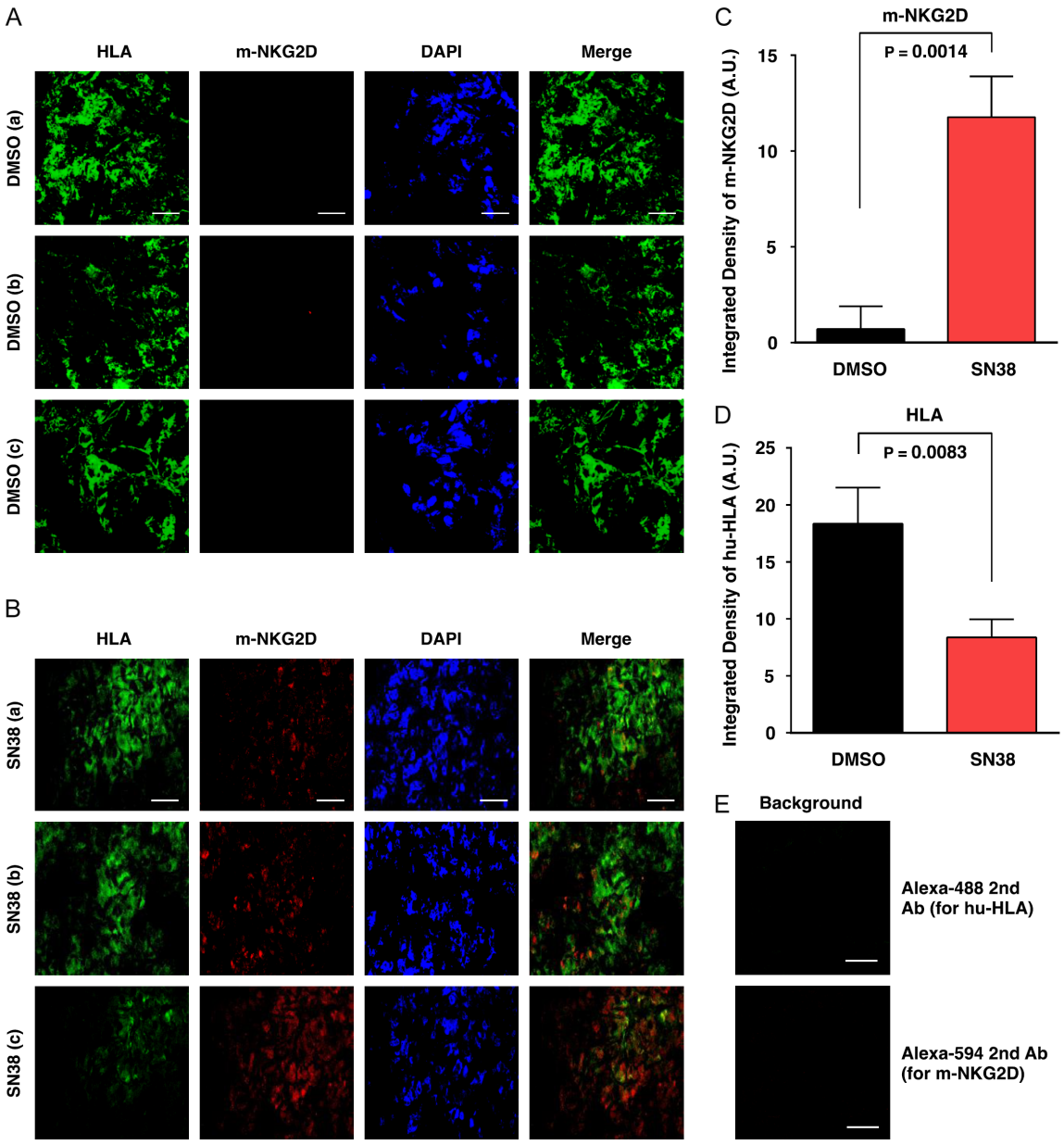

Figure 5. Low-dose SN38 recruits mouse NKG2D-positive NK cells into the TME of the primary OVCA429 tumors. We prepared the tumor slides as described above (**Figure 3B**). (A) Three slides of samples from OVCA429 tumors treated with DMSO were incubated with anti-human leukocyte antigen (HLA) or anti-mouse NKG2D (m-NKG2D) antibodies, followed by an Alexa Fluor 488- or 594-conjugated secondary antibodies and FCM. We utilized DAPI to show the nuclei. Scale bar: 20 μm. (B) Similarly, we incubated three slides of SN38-treated tumor samples with anti-HLA or anti-m-NKG2D antibodies and analyzed the stained cells as described above. (C, D) We show the relative expressions of m-NKG2D (C) and HLA (D) between tumors treated with DMSO and SN38 *in vivo* in the indicated histograms. (E) As negative antibody controls, slides of tumor specimens treated with DMSO (as described above) were incubated with an Alexa Fluor 488- or 594-conjugated secondary antibody only and analyzed by FCM.

(**Figure 9E**). Together, these results suggest that reducing STAT3, IL-6, c-Myc, and PD-L1 signaling in tumors may contribute to low-dose SN38-mediated antitumor immune response and tumor suppression *in vivo*.

Discussion

NK cells are vital cytotoxic lymphocytes crucial for the innate immune system. Recent findings have revealed a great deal of information about

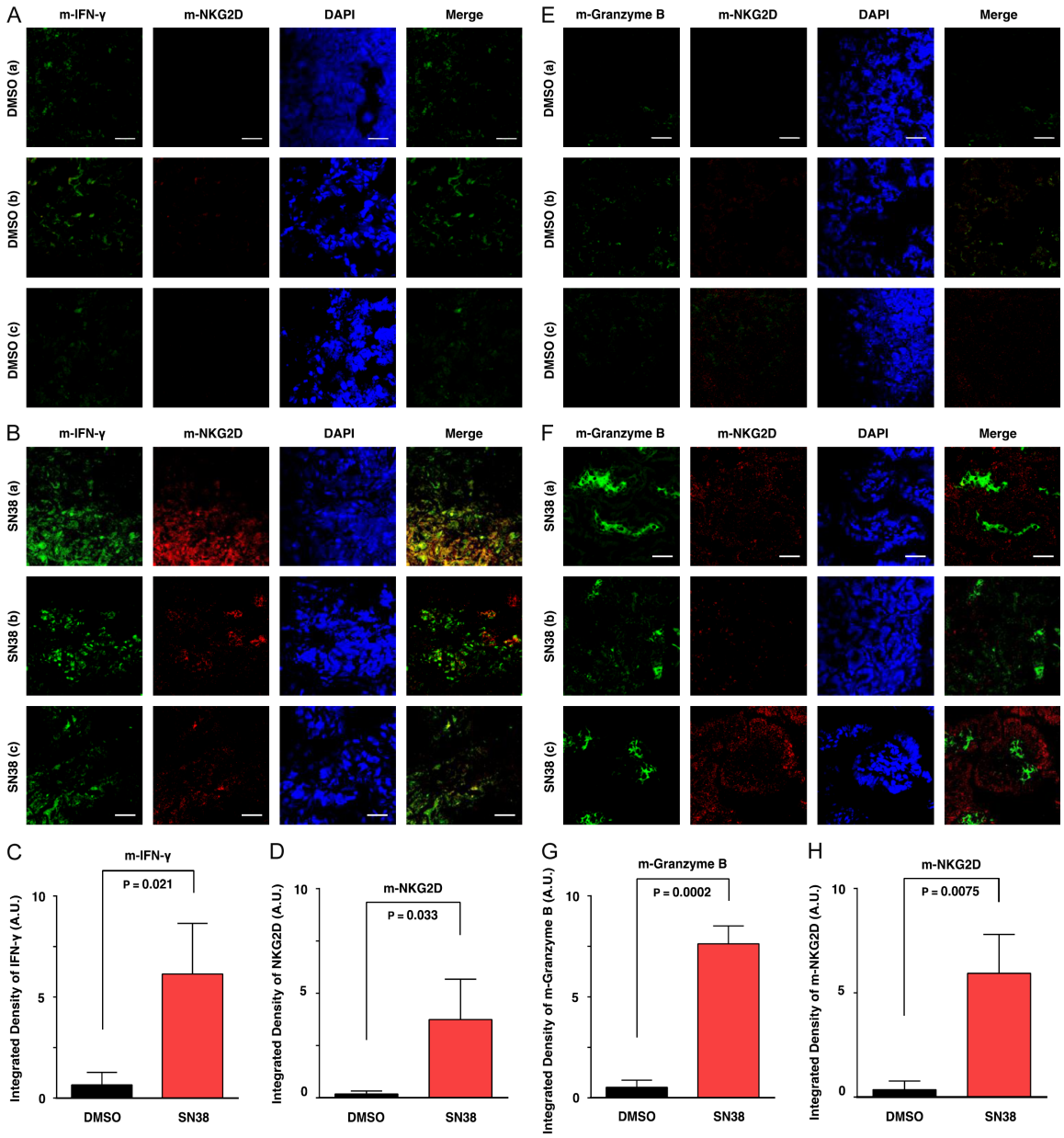

Figure 6. SN38 significantly increased mouse IFN-γ and granzyme B protein levels in the tumor microenvironment (TME) of the OVCA429 cancer mouse model. We prepared the tumor slides as described above (**Figure 3B**). (A, B) Three slides of samples from OVCA429 tumors treated with DMSO (A) or SN38 (B) were incubated with an anti-mouse antibody against mouse IFN-γ (m-IFN-γ) or m-NKG2D, followed by an Alexa Fluor 488- or 594-conjugated secondary antibodies and FCM. We utilized DAPI to show the nuclei. Scale bar: 20 μm. (C, D) We show the relative expressions of m-IFN-γ (C) and m-NKG2D (D) between tumors treated with DMSO and SN38 *in vivo* in the histograms as indicated, respectively. (E, F) Similarly, three slides of samples from tumors treated with DMSO (E) or SN38 (F) were incubated with an anti-mouse antibody against mouse granzyme B (m-granzyme B) or m-NKG2D, and the stained cells were analyzed as described above. (G, H) We display the relative expression of m-granzyme B (G) or m-NKG2D (H) between tumors treated with DMSO and SN38 *in vivo* in the histogram as indicated.

activating and inhibitory receptors of NK cells; however, it is still unclear how NK cells are explicitly regulated to target and kill tumor cells in the TME. Notably, emerging discoveries suggest that NK cells play a critical role in regulating cancer immunotherapy [36, 37]. However, the regulatory mechanisms controlling NK cells-mediated anticancer immune responses

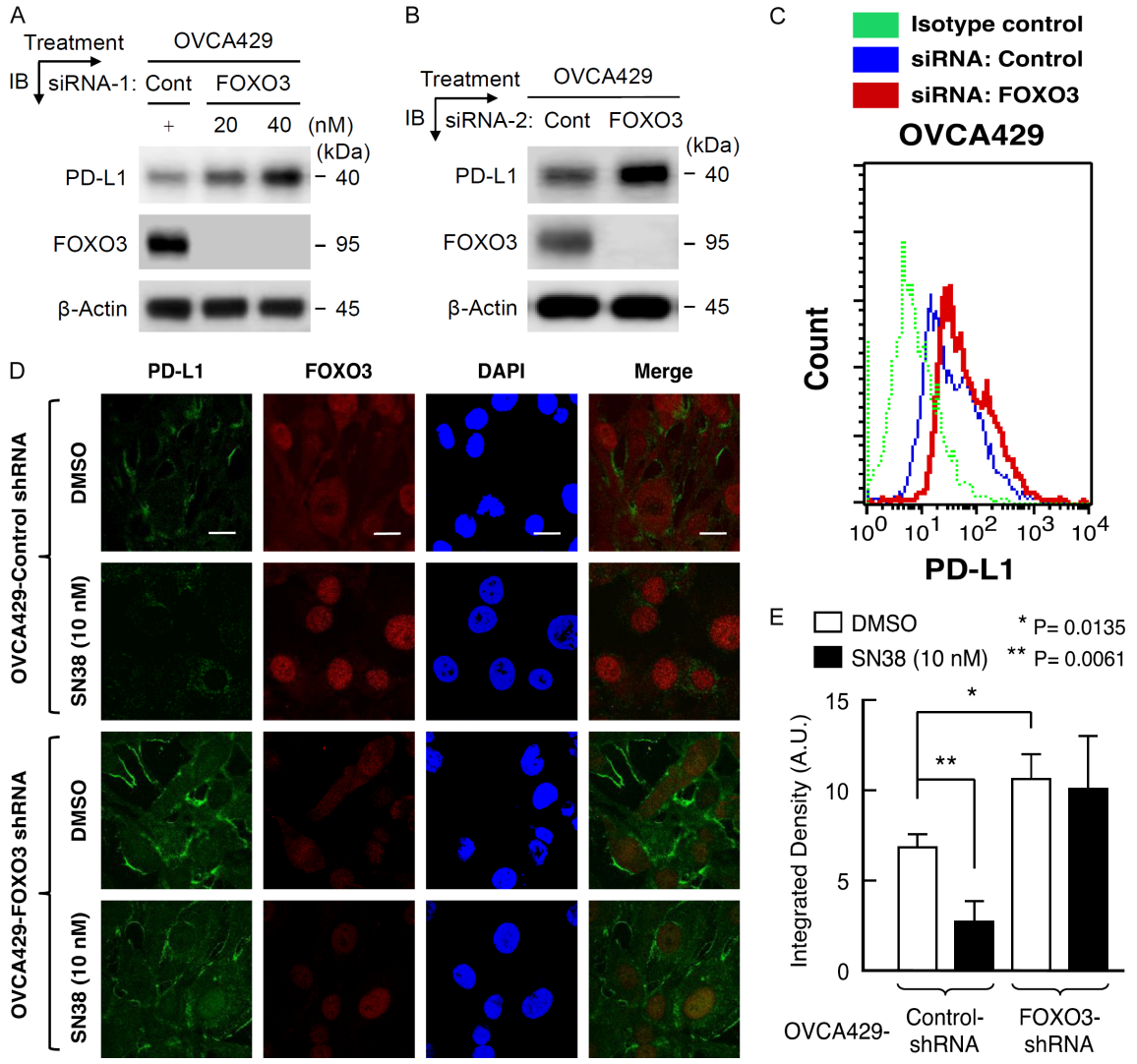

Figure 7. Silencing FOXO3 upregulates PD-L1 expression, and FOXO3 is essential for SN38-mediated downregulation of PD-L1 expression in tumor cells. (A, B) Human OVCA429 cells were transfected with specific siRNA-1 (A) or siRNA-2 (B) targeting human FOXO3 or control (cont) siRNA (as described in Methods and materials). We detected PD-L1 and FOXO3 Protein expressions in the total lysates of these cells using immunoblotting (IB) with the indicated Abs, and β-actin represents loading controls. (C) We transfected OVCA429 cells with specific siRNA-1 targeting human FOXO3 or control siRNA and analyzed these cells using flow cytometry with the designated antibodies or isotype IgG control. (D) We treated the OVCA429-Control-shRNA and -FOXO3-shRNA stable tumor cell lines (as described in Materials and methods) with low-dose SN38 (10 nM) or DMSO control. We incubated three slides of these SN38-treated cells with anti-PD-L1 (MAB1561, R&D Systems) and anti-FOXO3a (FKHRL1) (N-16, sc-9813, Santa Cruz Biotech) antibodies and followed by an Alexa Fluor 488- or 594-conjugated secondary antibodies and FCM as described above. (E) We exhibit the percentages of PD-L1 protein-positive cells in the histogram (three randomly captured images).

remain largely unknown. The present study shows that low-dose immunoactivators (e.g., SN38, topotecan, sorafenib, etc.) downregulate PD-L1 and upregulate FOXO3 expression in various cancer cell lines. In a mouse tumor model, low-dose SN38 treatments markedly suppress tumor growth, reduce PD-L1 expression, and enhance FOXO3 expression in primary tumor specimens. Low-dose SN38 therapy engages the tumor-infiltrating mouse NK1.1/CD49b/NKG2D-positive NK cells to attack tumor cells by inducing mouse IFN-γ and granzyme-B secretion in the tumor microenvironment (TME) *in vivo*. Our findings suggest a plausible thera-

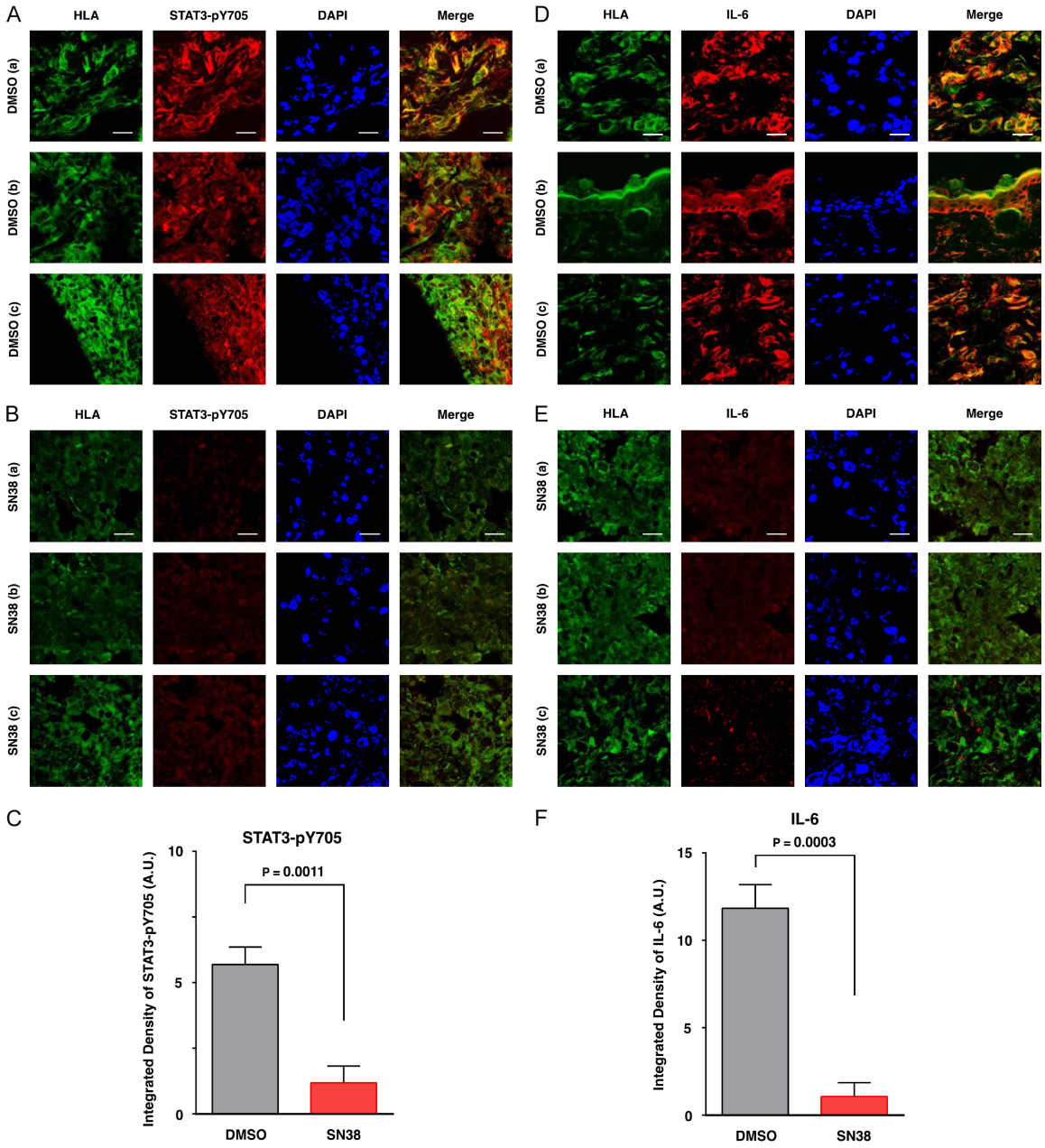

Figure 8. Low-dose SN38 treatment significantly reduces STAT3-pY705 and interleukin-6 (IL-6) protein levels in human OVCA429 tumor specimens. We prepared the tumor slides as described above (**Figure 3B**). (A) We incubated three slides of DMSO-treated OVCA429 tumor samples with an anti-human antibody against HLA or STAT3-pY705, followed by an Alexa Fluor 488- or 594-conjugated secondary antibodies and FCM. We utilized DAPI to show the nuclei. Scale bar: 20 μm. (B) Similarly, we incubated three slides of low-dose SN38-treated tumor specimens with an anti-human antibody against HLA or STAT3-pY705 and analyzed the stained cells as described above. (C) We show the relative expressions of STAT3-pY705 between tumors treated with DMSO and SN38 *in vivo* in the indicated histogram. (D, E) We incubated three slides of samples from OVCA429 tumors treated with DMSO (D) or SN38 (E) with an anti-human antibody against HLA or IL-6 and analyzed the stained cells as described above. (F) We demonstrate the relative expressions of IL-6 between tumors treated with DMSO and SN38 *in vivo* in the indicated histogram.

peutic tactic to activate NK cells for boosting cancer immunotherapy (e.g., ICBs) using low-dose immunoactivators (e.g., SN38, topotecan, etc.) without significant toxicity.

Resistance or unresponsiveness to available cancer immunotherapies (e.g., ICBs) may cause significant challenges to the treatment options for patients with difficult-to-treat cancers such

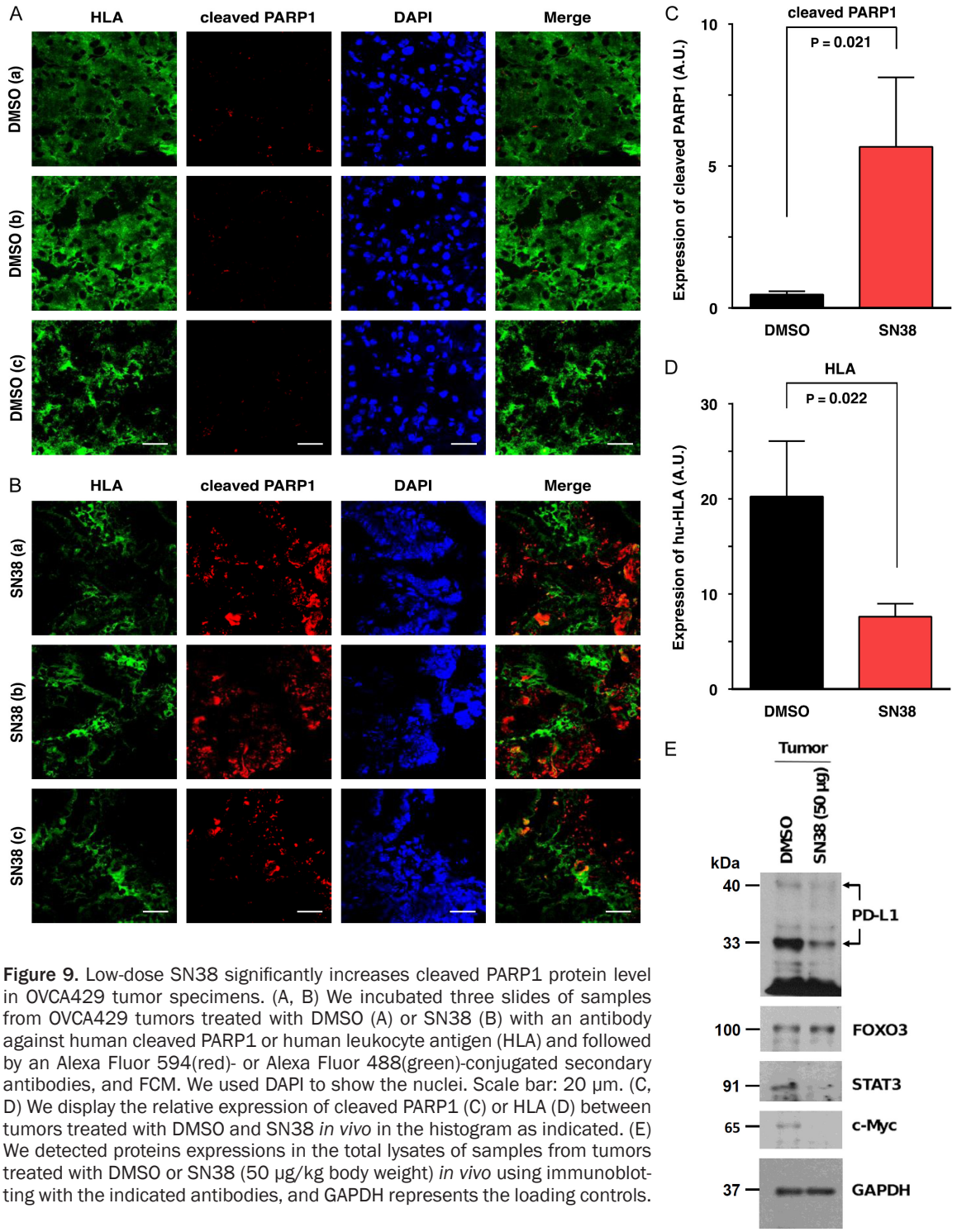

Figure 9. Low-dose SN38 significantly increases cleaved PARP1 protein level in OVCA429 tumor specimens. (A, B) We incubated three slides of samples from OVCA429 tumors treated with DMSO (A) or SN38 (B) with an antibody against human cleaved PARP1 or human leukocyte antigen (HLA) and followed by an Alexa Fluor 594(red)- or Alexa Fluor 488(green)-conjugated secondary antibodies, and FCM. We used DAPI to show the nuclei. Scale bar: 20 μm. (C, D) We display the relative expression of cleaved PARP1 (C) or HLA (D) between tumors treated with DMSO and SN38 *in vivo* in the histogram as indicated. (E) We detected proteins expressions in the total lysates of samples from tumors treated with DMSO or SN38 (50 μg/kg body weight) *in vivo* using immunoblotting with the indicated antibodies, and GAPDH represents the loading controls.

as OvCa. Activation of the PI3K/Akt, c-Myc, HIF-1α, or STAT3 cancer-promoting pathways can potently induce PD-L1 expression in tumor cells to trigger the hallmark immune evasion mechanism [38], which may lead to resistance or unresponsiveness to PD-L1/PD-1 ICBs. Small-molecule (SM) drugs can modulate oncogenic signaling pathways responsible for immune evasion mechanisms towards effective antitumor responses. Thus, the use of SM drugs to target oncogenic pathways may be an integral approach to enhancing the therapeutic effect

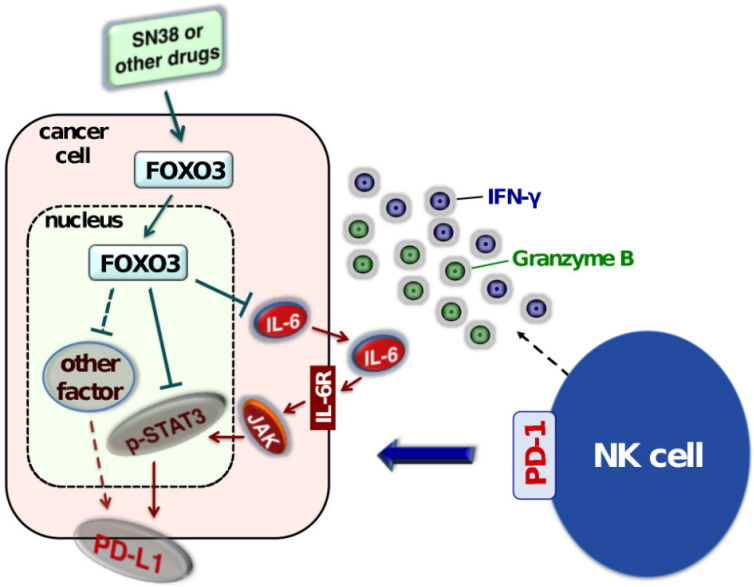

Figure 10. A schematic presentation illustrates a proposed model for the signaling mechanism underlying the FOXO3-dependent SN38- or other drug-mediated activation of NK cell anticancer immunity. This model illustrates that SN38 or other drugs can suppress the oncogenic pSTAT3, IL-6 (or other factors), and PD-L1 signaling pathways in cancer cells through FOXO3 and induce IFN-γ and granzyme B cytotoxic proteins in the TME to trigger NK cell killing of cancer cells.

of ICBs on cancer immunotherapy [39]. Indeed, our results show that low-dose SN38 drug markedly reduces PD-L1 protein levels and increases FOXO3 tumor suppressor protein levels in tumor cells, resulting in enhancing anti-PD-1 antitumor efficacy. Silencing FOXO3 expression in tumor cells revokes the SN38-mediated suppression of PD-L1 protein expression (**Figure 7**). In addition to PD-L1, our findings suggest that low-dose SN38 downregulates the levels of phosphorylated STAT3-pY705 (pSTAT3), IL-6, and c-Myc in human tumor cells. On the other hand, low-dose SN38 potently promotes IFN-γ and granzyme B protein levels in the TME. Overall, we have collectively proposed a schematic representation of a working model where low-dose SN38 or other immune-activating drugs can suppress the oncogenic STAT3, IL-6, c-Myc, and PD-L1 signaling pathways via a FOXO3-dependent mechanism in human tumor cells (**Figure 10**). In addition, our model suggests that low-dose SN38 or other drugs can induce IFN-γ and granzyme B cytotoxic proteins in the TME to trigger NK cell killing of tumors (**Figure 10**). NK cells release the content of cytolytic granules and secretion of factors such as chemokines and cytokines [40, 41], leading to the death of target cells. Among the secreted factors, IFN-γ is a key factor that plays a critical role in inducing NK cell or CD8+ T cell trafficking into the TME and boosting tumor cell killing [42]. Among granzymes and perforin in cytolytic granules, granzyme B is a key enzyme that plays a critical role in inducing the death of cancer cells. Indeed, our findings suggest that low-dose SN38 engages NK cell infiltration into the TME and triggers secretion of IFN-γ, which is detected in the adjacent area of NKG2D+ NK cells (**Figure 6**). Other than NK cells, activated T cells or other immune cells can also secret IFN-γ [42, 43]. A novel discovery indicates that lacking IFN-γ signaling genes in cancer cells is associated with cancer patients' resistance to CTLA-4 blockade treatment [44]. This report implies that deletions or mutations of the IFN-γ pathway genes may be valuable predictors for patients' resistance or responsiveness to particular ICB immunotherapy because the IFN-γ pathway is crucial for specific ICB clinical responses. This publication further supports our SN38-mediated antitumor immunomodulating model by triggering NK cells secreting IFN-γ to strengthen clinical responses to particular ICB therapy.

The oncogenic c-Myc protein plays a key role in regulating tumor growth and coordinating cellular adaptations in the TME and the prevention of the host antitumor immunity [45]. Notably, c-Myc overexpression is markedly correlated with PD-L1 expression in primary tumors and poor survival in patients with lung cancer [31]. We have previously shown that SN38 inhibits c-Myc protein expression in tumor cells in a FOXO3-dependent manner [22]. Thus, our findings imply that the SN38-mediated suppression of c-Myc protein expression may play an important role in PD-L1 downregulation in tumor cells in a FOXO3-dependent fashion. This notion is supported by a report showing that FOXO3 activation increases c-Myc phosphory-

lation and reduces c-Myc protein stability by FBW7-mediated ubiquitination and proteasomal degradation [46]. In addition to c-Myc, our results suggest that the SN38-mediated decrease of pSTAT3 and IL-6 protein levels may be crucial for reducing PD-L1 expression in tumor cells. This implication is supported by several reports indicating that the IL-6/JAK/STAT3 signaling pathway has a vital role in the upregulation of PD-L1 expression [32, 33], and targeting the IL-6/JAK/STAT3 pathway by their inhibitors can stimulate antitumor immunity [47]. Furthermore, it has been shown that upregulated HIF-1α expression is associated with enhanced PD-L1 expression in tumor cells and cause suppression of T-cell function in the TME [48, 49], suggesting that increased HIF-1α expression under hypoxic conditions may lead to immunosuppression in the TME. Interestingly, SN38 or irinotecan has been found to suppress HIF-1α in tumor cells [50, 51]. These findings support our proposed model of using SN38 to boost antitumor immune responses by suppressing oncogenic signaling pathways in tumor cells.

Nonetheless, the detailed molecular mechanisms underpinning the SN38- or other immunoactivators-mediated anticancer immunity *in vivo* remain largely unclear and will be elucidated further. For instance, several literature findings have shown compelling evidence to reveal that suppressing PD-L1 expression on cancer cells directly by small-molecule medicines or indirectly by silencing PD-L1's upstream target genes results in boosting anticancer immune responses [52-61]. A plausible mechanism for this small-molecule immunoactivator (e.g., SN38)-mediated reducing PD-L1 expression and increasing anticancer immune response should be similar to an anti-PD-L1 blockade that inhibits the PD-1/PD-L1 checkpoint interaction. Another likely mechanism for SN38-promoted anticancer immune response is that SN38 treatment triggers NK cell recruitment into the TME. Our findings support this mechanism showing few infiltrated NK cells or T cells in the TME of the primary tumors without SN38 treatment (**Figures 4** and **5**). In contrast, our results reveal markedly increased numbers of engaged NK cells infiltrating the TME *in vivo* in the presence of SN38 (**Figures 4** and **5**). Furthermore, it is possible that small-molecule drugs (e.g., SN38)-mediated suppression of PD-L1 expression to enhance anticancer immune response through reducing infiltration of immunosuppressive immune cells (e.g., macrophages or regulatory T cells or myeloid-derived suppressor cells) into the TME. Emerging findings of small-molecule medicine lenvatinib-mediated ameliorating antitumor immune response have suggested this new mechanism [62, 63]. However, we cannot rule out other potential mechanisms. In contrast, certain novel findings have shown that specific targeted therapeutics or chemotherapeutic drugs can upregulate PD-L1 expression in tumor cells and increase a PD-L1 blockade-mediated antitumor immune response [64, 65]. However, the prospective mechanisms for these phenomena appear different from the SN38-mediated signaling pathways (as described above). For instance, when tumor cells express low or insignificant levels of PD-L1 proteins, the tumor immune escapes seem not to depend on the PD1/PD-L1 checkpoint signaling, resulting in resistance or unresponsiveness to PD1 or PD-L1 checkpoint blockades. Their tumor immune escapes may rely on alternative immune checkpoint mechanisms (CTLA4/CD80/86, TIM-3/galectin-9, etc.). When specific compound drugs constitutively upregulate PD-L1 expression in the PD1 or PD-L1 blockade-resistant tumor cells, their tumor immune escapes may acquire a dependence on the PD1/PD-L1 checkpoint signaling and enhance responsiveness to PD1 or PD-L1 checkpoint blockade therapy. However, various compound immunoactivators' regulatory mechanisms for ameliorating anticancer immunity seem complex and remain further deciphered in the future.

Although our mouse tumor model is not a syngeneic mouse tumor model, our *in vivo* system provides certain advantages over a syngeneic system. (1) Our new findings are based on human cancer cells, whereas most results obtained from known syngeneic mouse tumor models are based on mouse cancer cells. Although the immune system appears conserved between humans and mice, the complex immune regulatory mechanisms may not be identical between humans and mice. In particular, several regulatory receptors or factors expressed in NK cells seem distinct between humans and mice. For instance, human NK cells express natural cytotoxicity receptors (e.g., NKp30, NKp44, and NKp46) on the cell

surface, whereas mouse NK cells express mainly NKp46 and do not express NKp30 [66]. Human NK cells express CD56 receptors on the cell surface abundantly, but mouse NK cells do not express CD56 receptors [67]. (2) In the immunocompetent mice, NK cell proliferation and activity are controlled by regulatory T cells via regulating the secretion of a vital cytokine IL-2, which controls NK cell proliferation [68], and a negative cytokine transforming growth factor-β, which inhibits NK cell functions [68]. Moreover, circulating lymphocytes comprise approximately 85% T cell populations [69], much more abundant than 2-5% NK cell populations [70] in immunocompetent mice. Thus, the unique roles of NK cells in regulating tumor cell survival and tumor progression in the TME may be constrained or masked by various T cells in the immunocompetent mice. Our new findings are based on human cancer cells in the immunocompromised nude mice, which lack mature functional T cells [71]. In addition, nude mice have preserved functional NK cells or more NK cells than the immunocompetent mice to compensate for their lack of active mature T cells [72, 73]. Thus, our mouse system may work as an animal model of impaired T-cell function with mature T cells depleted to show NK cell function and activity more clearly than the immunocompetent mice.

Regarding overarching cancer immunotherapy strategies, our current SN38-NK cell findings may contribute to advancing integrated immune-activating medicines (e.g., SN38 or topotecan, etc.) with ICB immunotherapy to boost the optimal therapeutic efficacy for saving lives of patients suffering from difficult-to-treat cancers. Strikingly, Sun et al. have discovered crucial adaptive immune features of NK cells [74]. Krebs et al. have revealed that NK-cell-mediated elimination of target cells can trigger strong antigen-specific CD8+ T-cell-mediated adaptive immunity and humoral response [75]. In addition, recent findings indicated that SN38 inhibits lipopolysaccharide (LPS)-mediated toll-like receptor 4 (TLR4) signaling in macrophages, resulting in suppressing the acute inflammatory response [76]. Notably, topoisomerase-I (Top-I) inhibitors have been shown to prevent LPS-induced death in animals by suppressing the inflammatory genes [77]. Together, our findings suggest that low-dose SN38 and topotecan (Top-I inhibitors) or other immunoactivators may significantly improve anticancer immune response and mitigate potential adverse side effects by abrogating the acute inflammatory response in cancer patients concurrently. However, it is unclear whether low-dose SN38 or topotecan may regulate other gene expressions in cancer cells or other immune cells in the TME to contribute to the observed anti-tumor immune response *in vivo*. Hence, further investigation of the role and mechanism of low-dose immune activators (e.g., SN38, topotecan, etc.) in inhibiting the acute inflammatory responses is necessary to facilitate immune activators-enhanced ICB-mediated cancer immunotherapy while thwarting intolerable side effects. In general, the scope of immune-activating drugs in promoting NK-mediated tumor suppression may be a common property applicable to certain small-molecule drugs. Finally, it is plausible to evaluate further this promising strategy to overcome ICB-resistant or intractable cancers with SN38 or topotecan or other immune-activating drugs to boost ICB therapeutic efficacy and optimize therapeutic applications of effective combination therapies for overcoming life-threatening cancers in the future.

Acknowledgements

This study was funded in part by grants 1R21CA201940-01A1 and 1R41CA183335-01 from the National Cancer Institute, National Institutes of Health (to M.C.T.H.), grants W81XWH2010883, W81XWH2010398, and W81XWH2010260 from the Department of Defense, Congressionally Directed Medical Research Programs (to M.C.T.H.), and grants 02-2013-051 and 02-2017-067 from the Avon Foundation for Women (to M.C.T.H.). We thank Yanli Qiao for her excellent technical support and Oliver Dorigo, Robert C. Bast, Jr., and Xiaoyuan (Shawn) Chen for generously providing reagents. The sponsors had no role in the study's design, conduct, or reporting.

Disclosure of conflict of interest

None.

Address correspondence to: Mickey C-T Hu, Panorama Institute of Molecular Medicine & Panorama Research Institute, Sunnyvale, CA 94089, USA. E-mail: mhu1stanfored@gmail.com

References

[1] Topalian SL, Drake CG and Pardoll DM. Immune checkpoint blockade: a common denominator approach to cancer therapy. Cancer Cell 2015; 27: 450-461.

[2] Zou W, Wolchok JD and Chen L. PD-L1 (B7-H1) and PD-1 pathway blockade for cancer therapy: mechanisms, response biomarkers, and combinations. Sci Transl Med 2016; 8: 328rv324.

[3] Brahm CG, van Linde ME, Enting RH, Schuur M, Otten RHJ, Heymans MW, Verheul HMW and Walenkamp AME. The current status of immune checkpoint inhibitors in neuro-oncology: a systematic review. Cancers (Basel) 2020; 12: 586.

[4] O'Reilly EM, Oh DY, Dhani N, Renouf DJ, Lee MA, Sun W, Fisher G, Hezel A, Chang SC, Vlahovic G, Takahashi O, Yang Y, Fitts D and Philip PA. Durvalumab with or without tremelimumab for patients with metastatic pancreatic ductal adenocarcinoma: a phase 2 randomized clinical trial. JAMA Oncol 2019; 5: 1431-1438.

[5] Melzer MK, Arnold F, Stifter K, Zengerling F, Azoitei N, Seufferlein T, Bolenz C and Kleger A. An immunological glance on pancreatic ductal adenocarcinoma. Int J Mol Sci 2020; 21: 3345.

[6] Doo DW, Norian LA and Arend RC. Checkpoint inhibitors in ovarian cancer: a review of preclinical data. Gynecol Oncol Rep 2019; 29: 48-54.

[7] Hewitt EW. The MHC class I antigen presentation pathway: strategies for viral immune evasion. Immunology 2003; 110: 163-169.

[8] Kobayashi KS and van den Elsen PJ. NLRC5: a key regulator of MHC class I-dependent immune responses. Nat Rev Immunol 2012; 12: 813-820.

[9] Sade-Feldman M, Jiao YJ, Chen JH, Rooney MS, Barzily-Rokni M, Eliane JP, Bjorgaard SL, Hammond MR, Vitzthum H, Blackmon SM, Frederick DT, Hazar-Rethinam M, Nadres BA, Van Seventer EE, Shukla SA, Yizhak K, Ray JP, Rosebrock D, Livitz D, Adalsteinsson V, Getz G, Duncan LM, Li B, Corcoran RB, Lawrence DP, Stemmer-Rachamimov A, Boland GM, Landau DA, Flaherty KT, Sullivan RJ and Hacohen N. Resistance to checkpoint blockade therapy through inactivation of antigen presentation. Nat Commun 2017; 8: 1136.

[10] Sharma P, Kumar P and Sharma R. Natural Killer Cells - Their role in tumour immunosurveillance. J Clin Diagn Res 2017; 11: BE01-BE05.

[11] Shifrin N, Raulet DH and Ardolino M. NK cell self tolerance, responsiveness and missing self recognition. Semin Immunol 2014; 26: 138-144.

[12] Raulet DH. Missing self recognition and self tolerance of natural killer (NK) cells. Semin Immunol 2006; 18: 145-150.

[13] Martin-Fontecha A, Thomsen LL, Brett S, Gerard C, Lipp M, Lanzavecchia A and Sallusto F. Induced recruitment of NK cells to lymph nodes provides IFN-gamma for T(H)1 priming. Nat Immunol 2004; 5: 1260-1265.

[14] Trinchieri G. Biology of natural killer cells. Adv Immunol 1989; 47: 187-376.

[15] Miller JS and Lanier LL. Natural killer cells in cancer immunotherapy. Annu Rev Cancer Biol 2019; 3: 77-103

[16] Kaiser BK, Pizarro JC, Kerns J and Strong RK. Structural basis for NKG2A/CD94 recognition of HLA-E. Proc Natl Acad Sci U S A 2008; 105: 6696-6701.

[17] Simon S and Labarriere N. PD-1 expression on tumor-specific T cells: friend or foe for immunotherapy? Oncoimmunology 2017; 7: e1364828.

[18] Huang BY, Zhan YP, Zong WJ, Yu CJ, Li JF, Qu YM and Han S. The PD-1/B7-H1 pathway modulates the natural killer cells versus mouse glioma stem cells. PLoS One 2015; 10: e0134715.

[19] Hsu J, Hodgins JJ, Marathe M, Nicolai CJ, Bourgeois-Daigneault MC, Trevino TN, Azimi CS, Scheer AK, Randolph HE, Thompson TW, Zhang L, Iannello A, Mathur N, Jardine KE, Kirn GA, Bell JC, McBurney MW, Raulet DH and Ardolino M. Contribution of NK cells to immunotherapy mediated by PD-1/PD-L1 blockade. J Clin Invest 2018; 128: 4654-4668.

[20] Paul S and Lal G. The molecular mechanism of natural killer cells function and its importance in cancer immunotherapy. Front Immunol 2017; 8: 1124.

[21] Ben-Shmuel A, Biber G and Barda-Saad M. Unleashing natural killer cells in the tumor microenvironment-the next generation of immunotherapy? Front Immunol 2020; 11: 275.

[22] Hu T, Chung YM, Guan M, Ma M, Ma J, Berek JS and Hu MC. Reprogramming ovarian and breast cancer cells into non-cancerous cells by low-dose metformin or SN-38 through FOXO3 activation. Sci Rep 2014; 4: 5810.

[23] Greer EL and Brunet A. FOXO transcription factors at the interface between longevity and tumor suppression. Oncogene 2005; 24: 7410-7425.

[24] Fu Z and Tindall DJ. FOXOs, cancer and regulation of apoptosis. Oncogene 2008; 27: 2312-2319.

[25] Yang JY and Hung MC. A new fork for clinical application: targeting forkhead transcription factors in cancer. Clin Cancer Res 2009; 15: 752-757.

[26] Hu MC, Lee DF, Xia W, Golfman LS, Ou-Yang F, Yang JY, Zou Y, Bao S, Hanada N, Saso H, Kobayashi R and Hung MC. IkappaB kinase promotes tumorigenesis through inhibition of forkhead FOXO3a. Cell 2004; 117: 225-237.
[27] Tsai WB, Chung YM, Takahashi Y, Xu Z and Hu MC. Functional interaction between FOXO3a and ATM regulates DNA damage response. Nat Cell Biol 2008; 10: 460-467.
[28] Chung YM, Park SH, Tsai WB, Wang SY, Ikeda MA, Berek JS, Chen DJ and Hu MC. FOXO3 signalling links ATM to the p53 apoptotic pathway following DNA damage. Nat Commun 2012; 3: 1000.
[29] Audesse AJ, Dhakal S, Hassell LA, Gardell Z, Nemtsova Y and Webb AE. FOXO3 directly regulates an autophagy network to functionally regulate proteostasis in adult neural stem cells. PLoS Genet 2019; 15: e1008097.
[30] Park SH, Chung YM, Ma J, Yang Q, Berek JS and Hu MC. Pharmacological activation of FOXO3 suppresses triple-negative breast cancer in vitro and in vivo. Oncotarget 2016; 7: 42110-42125.
[31] Kim EY, Kim A, Kim SK and Chang YS. MYC expression correlates with PD-L1 expression in non-small cell lung cancer. Lung Cancer 2017; 110: 63-67.
[32] Bu LL, Yu GT, Wu L, Mao L, Deng WW, Liu JF, Kulkarni AB, Zhang WF, Zhang L and Sun ZJ. STAT3 induces immunosuppression by upregulating PD-1/PD-L1 in HNSCC. J Dent Res 2017; 96: 1027-1034.
[33] Atsaves V, Tsesmetzis N, Chioureas D, Kis L, Leventaki V, Drakos E, Panaretakis T, Grander D, Medeiros LJ, Young KH and Rassidakis GZ. PD-L1 is commonly expressed and transcriptionally regulated by STAT3 and MYC in ALK-negative anaplastic large-cell lymphoma. Leukemia 2017; 31: 1633-1637.
[34] Kaufmann SH, Desnoyers S, Ottaviano Y, Davidson NE and Poirier GG. Specific proteolytic cleavage of poly(ADP-ribose) polymerase: an early marker of chemotherapy-induced apoptosis. Cancer Res 1993; 53: 3976-3985.
[35] Tewari M, Quan LT, O'Rourke K, Desnoyers S, Zeng Z, Beidler DR, Poirier GG, Salvesen GS and Dixit VM. Yama/CPP32 beta, a mammalian homolog of CED-3, is a CrmA-inhibitable protease that cleaves the death substrate poly(ADP-ribose) polymerase. Cell 1995; 81: 801-809.
[36] Romee R, Rosario M, Berrien-Elliott MM, Wagner JA, Jewell BA, Schappe T, Leong JW, Abdel-Latif S, Schneider SE, Willey S, Neal CC, Yu L, Oh ST, Lee YS, Mulder A, Claas F, Cooper MA and Fehniger TA. Cytokine-induced memory-like natural killer cells exhibit enhanced responses against myeloid leukemia. Sci Transl Med 2016; 8: 357ra123.
[37] Uppendahl LD, Felices M, Bendzick L, Ryan C, Kodal B, Hinderlie P, Boylan KLM, Skubitz APN, Miller JS and Geller MA. Cytokine-induced memory-like natural killer cells have enhanced function, proliferation, and in vivo expansion against ovarian cancer cells. Gynecol Oncol 2019; 153: 149-157.
[38] Hanahan D and Weinberg RA. Hallmarks of cancer: the next generation. Cell 2011; 144: 646-674.
[39] van der Zanden SY, Luimstra JJ, Neefjes J, Borst J and Ovaa H. Opportunities for small molecules in cancer immunotherapy. Trends Immunol 2020; 41: 493-511.
[40] Gwalani LA and Orange JS. Single degranulations in NK cells can mediate target cell killing. J Immunol 2018; 200: 3231-3243.
[41] Hsu HT, Mace EM, Carisey AF, Viswanath DI, Christakou AE, Wiklund M, Önfelt B and Orange JS. NK cells converge lytic granules to promote cytotoxicity and prevent bystander killing. J Cell Biol 2016; 215: 875-889.
[42] Castro F, Cardoso AP, Gonçalves RM, Serre K and Oliveira MJ. Interferon-gamma at the crossroads of tumor immune surveillance or evasion. Front Immunol 2018; 9: 847.
[43] Tau G and Rothman P. Biologic functions of the IFN-gamma receptors. Allergy 1999; 54: 1233-1251.
[44] Gao J, Shi LZ, Zhao H, Chen J, Xiong L, He Q, Chen T, Roszik J, Bernatchez C, Woodman SE, Chen PL, Hwu P, Allison JP, Futreal A, Wargo JA and Sharma P. Loss of IFN-gamma pathway genes in tumor cells as a mechanism of resistance to anti-CTLA-4 therapy. Cell 2016; 167: 397-404, e399.
[45] Gabay M, Li Y and Felsher DW. MYC activation is a hallmark of cancer initiation and maintenance. Cold Spring Harb Perspect Med 2014; 4: a014241.
[46] Ferber EC, Peck B, Delpuech O, Bell GP, East P and Schulze A. FOXO3a regulates reactive oxygen metabolism by inhibiting mitochondrial gene expression. Cell Death Differ 2012; 19: 968-979.
[47] Johnson DE, O'Keefe RA and Grandis JR. Targeting the IL-6/JAK/STAT3 signalling axis in cancer. Nat Rev Clin Oncol 2018; 15: 234-248.
[48] Barsoum IB, Smallwood CA, Siemens DR and Graham CH. A mechanism of hypoxia-mediated escape from adaptive immunity in cancer cells. Cancer Res 2014; 74: 665-674.
[49] Noman MZ, Desantis G, Janji B, Hasmim M, Karray S, Dessen P, Bronte V and Chouaib S. PD-L1 is a novel direct target of HIF-1alpha, and its blockade under hypoxia enhanced MDSC-mediated T cell activation. J Exp Med 2014; 211: 781-790.
[50] Kamiyama H, Takano S, Tsuboi K and Matsumura A. Anti-angiogenic effects of SN38 (ac-

tive metabolite of irinotecan): inhibition of hypoxia-inducible factor 1 alpha (HIF-1alpha)/vascular endothelial growth factor (VEGF) expression of glioma and growth of endothelial cells. J Cancer Res Clin Oncol 2005; 131: 205-213.

[51] Murono K, Tsuno NH, Kawai K, Sasaki K, Hongo K, Kaneko M, Hiyoshi M, Tada N, Nirei T, Sunami E, Takahashi K and Kitayama J. SN-38 overcomes chemoresistance of colorectal cancer cells induced by hypoxia, through HIF1alpha. Anticancer Res 2012; 32: 865-872.

[52] Zhu H, Bengsch F, Svoronos N, Rutkowski MR, Bitler BG, Allegrezza MJ, Yokoyama Y, Kossenkov AV, Bradner JE, Conejo-Garcia JR and Zhang R. BET bromodomain inhibition promotes anti-tumor immunity by suppressing PD-L1 expression. Cell Rep 2016; 16: 2829-2837.

[53] Dorand RD, Nthale J, Myers JT, Barkauskas DS, Avril S, Chirieleison SM, Pareek TK, Abbott DW, Stearns DS, Letterio JJ, Huang AY and Petrosiute A. Cdk5 disruption attenuates tumor PD-L1 expression and promotes antitumor immunity. Science 2016; 353: 399-403.

[54] Taylor A, Rothstein D and Rudd CE. Small-molecule inhibition of PD-1 transcription is an effective alternative to antibody blockade in cancer therapy. Cancer Res 2018; 78: 706-717.

[55] Sun LL, Yang RY, Li CW, Chen MK, Shao B, Hsu JM, Chan LC, Yang Y, Hsu JL, Lai YJ and Hung MC. Inhibition of ATR downregulates PD-L1 and sensitizes tumor cells to T cell-mediated killing. Am J Cancer Res 2018; 8: 1307-1316.

[56] Zou MZ, Liu WL, Li CX, Zheng DW, Zeng JY, Gao F, Ye JJ and Zhang XZ. A multifunctional biomimetic nanoplatform for relieving hypoxia to enhance chemotherapy and inhibit the PD-1/PD-L1 axis. Small 2018; 14: e1801120.

[57] Luo F, Luo M, Rong QX, Zhang H, Chen Z, Wang F, Zhao HY and Fu LW. Niclosamide, an antihelmintic drug, enhances efficacy of PD-1/PD-L1 immune checkpoint blockade in non-small cell lung cancer. J Immunother Cancer 2019; 7: 245.

[58] Liang J, Wang L, Wang C, Shen J, Su B, Marisetty AL, Fang D, Kassab C, Jeong KJ, Zhao W, Lu Y, Jain AK, Zhou Z, Liang H, Sun SC, Lu C, Xu ZX, Yu Q, Shao S, Chen X, Gao M, Claret FX, Ding Z, Chen J, Chen P, Barton MC, Peng G, Mills GB and Heimberger AB. Verteporfin inhibits PD-L1 through autophagy and the STAT1-IRF1-TRIM28 signaling axis, exerting antitumor efficacy. Cancer Immunol Res 2020; 8: 952-965.

[59] Munoz LE, Huang L, Bommireddy R, Sharma R, Monterroza L, Guin RN, Samaranayake SG, Pack CD, Ramachandiran S, Reddy SJC, Shanmugam M and Selvaraj P. Metformin reduces PD-L1 on tumor cells and enhances the anti-tumor immune response generated by vaccine immunotherapy. J Immunother Cancer 2021; 9: e002614.

[60] Ri MH, Ma J and Jin X. Development of natural products for anti-PD-1/PD-L1 immunotherapy against cancer. J Ethnopharmacol 2021; 281: 114370.

[61] Liu J, Chen Z, Li Y, Zhao W, Wu J and Zhang Z. PD-1/PD-L1 checkpoint inhibitors in tumor immunotherapy. Front Pharmacol 2021; 12: 731798.

[62] Yi C, Chen L, Lin Z, Liu L, Shao W, Zhang R, Lin J, Zhang J, Zhu W, Jia H, Qin L, Lu L and Chen J. Lenvatinib targets FGF receptor 4 to enhance antitumor immune response of anti-programmed cell death-1 in HCC. Hepatology 2021; 74: 2544-2560.

[63] Kato Y, Tabata K, Kimura T, Yachie-Kinoshita A, Ozawa Y, Yamada K, Ito J, Tachino S, Hori Y, Matsuki M, Matsuoka Y, Ghosh S, Kitano H, Nomoto K, Matsui J and Funahashi Y. Lenvatinib plus anti-PD-1 antibody combination treatment activates CD8+ T cells through reduction of tumor-associated macrophage and activation of the interferon pathway. PLoS One 2019; 14: e0212513.

[64] Jiao S, Xia W, Yamaguchi H, Wei Y, Chen MK, Hsu JM, Hsu JL, Yu WH, Du Y, Lee HH, Li CW, Chou CK, Lim SO, Chang SS, Litton J, Arun B, Hortobagyi GN and Hung MC. PARP inhibitor upregulates PD-L1 expression and enhances cancer-associated immunosuppression. Clin Cancer Res 2017; 23: 3711-3720.

[65] Peng J, Hamanishi J, Matsumura N, Abiko K, Murat K, Baba T, Yamaguchi K, Horikawa N, Hosoe Y, Murphy SK, Konishi I and Mandai M. Chemotherapy induces programmed cell death-ligand 1 overexpression via the nuclear factor-kappaB to foster an immunosuppressive tumor microenvironment in ovarian cancer. Cancer Res 2015; 75: 5034-5045.

[66] Barrow AD, Martin CJ and Colonna M. The natural cytotoxicity receptors in health and disease. Front Immunol 2019; 10: 909.

[67] Hayakawa Y, Huntington ND, Nutt SL and Smyth MJ. Functional subsets of mouse natural killer cells. Immunol Rev 2006; 214: 47-55.

[68] Kerdiles Y, Ugolini S and Vivier E. T cell regulation of natural killer cells. J Exp Med 2013; 210: 1065-1068.

[69] Sprent J and Basten A. Circulating T and B lymphocytes of the mouse. II. Lifespan. Cell Immunol 1973; 7: 40-59.

[70] Jiao Y, Huntington ND, Belz GT and Seillet C. Type 1 innate lymphoid cell biology: lessons learnt from natural killer cells. Front Immunol 2016; 7: 426.

[71] Pelleitier M and Montplaisir S. The nude mouse: a model of deficient T-cell function. Methods Achiev Exp Pathol 1975; 7: 149-166.
[72] Tsuchiyama T, Nakamoto Y, Sakai Y, Marukawa Y, Kitahara M, Mukaida N and Kaneko S. Prolonged, NK cell-mediated antitumor effects of suicide gene therapy combined with monocyte chemoattractant protein-1 against hepatocellular carcinoma. J Immunol 2007; 178: 574-583.
[73] Meyerrose TE, Herrbrich P, Hess DA and Nolta JA. Immune-deficient mouse models for analysis of human stem cells. Biotechniques 2003; 35: 1262-1272.
[74] Sun JC, Beilke JN and Lanier LL. Adaptive immune features of natural killer cells. Nature 2009; 457: 557-561.
[75] Krebs P, Barnes MJ, Lampe K, Whitley K, Bahjat KS, Beutler B, Janssen E and Hoebe K. NK-cell-mediated killing of target cells triggers robust antigen-specific T-cell-mediated and humoral responses. Blood 2009; 113: 6593-6602.
[76] Wong DVT, Ribeiro-Filho HV, Wanderley CWS, Leite CAVG, Lima JB, Assef ANB, Cajado AG, Batista GLP, González RH, Silva KO, Borges LPC, Alencar NMN, Wilke DV, Cunha TM, Figueira ACM, Cunha FQ and Lima-Júnior RCP. SN-38, the active metabolite of irinotecan, inhibits the acute inflammatory response by targeting toll-like receptor 4. Cancer Chemother Pharmacol 2019; 84: 287-298.
[77] Rialdi A, Campisi L, Zhao N, Lagda AC, Pietzsch C, Ho JSY, Martinez-Gil L, Fenouil R, Chen X, Edwards M, Metreveli G, Jordan S, Peralta Z, Munoz-Fontela C, Bouvier N, Merad M, Jin J, Weirauch M, Heinz S, Benner C, van Bakel H, Basler C, García-Sastre A, Bukreyev A and Marazzi I. Topoisomerase 1 inhibition suppresses inflammatory genes and protects from death by inflammation. Science 2016; 352: aad7993.